

A unified BFKL and GLAP description of F_2 data

J. Kwiecinski^{a,b}, A.D. Martin^a and A.M. Stasto^{a,b}

- ^a Department of Physics, University of Durham, Durham, DH1 3LE, UK.
^b H. Niewodniczanski Institute of Nuclear Physics, Department of Theoretical Physics,
ul. Radzikowskiego 152, 31-342 Krakow, Poland.

Abstract

We argue that the use of the universal *unintegrated* gluon distribution and the k_T (or high energy) factorization theorem provides the natural framework for describing observables at small x . We introduce a coupled pair of evolution equations for the unintegrated gluon distribution and the sea quark distribution which incorporate both the resummed leading $\ln(1/x)$ BFKL contributions and the resummed leading $\ln(Q^2)$ GLAP contributions. We solve these unified equations in the perturbative QCD domain using simple parametric forms of the nonperturbative part of the *integrated* distributions. With only two (physically motivated) input parameters we find that this k_T factorization approach gives an excellent description of the measurements of $F_2(x, Q^2)$ at HERA. In this way the unified evolution equations allow us to determine the gluon and sea quark distributions and, moreover, to see the x domain where the resummed $\ln(1/x)$ effects become significant. We use k_T factorization to predict the longitudinal structure function $F_L(x, Q^2)$ and the charm component of $F_2(x, Q^2)$.

1. Introduction

The experiments at HERA have opened up the small Bjorken x regime. One of the most striking features of the data is the strong rise of the structure function F_2 as x decreases from 10^{-2} to below 10^{-4} [1]. At first sight it appeared that the rise was due to the (BFKL) resummation of leading $\ln(1/x)$ contributions [2, 3]. However, with an appropriate choice of input distributions and of the starting scale for the Q^2 evolution, the observed growth can also be reproduced within the conventional GLAP framework which just sums up the leading (and next-to-leading) $\ln Q^2$ contributions. Indeed GLAP global fits exist which give a good description of the small x measurements of F_2 in the x range accessible at HERA [4, 5], see also [6, 7]. Is it possible to conclude that there will be no significant BFKL-type contributions to F_2 in the HERA small x regime or does a physically reasonable alternative description exist with sizeable $\ln(1/x)$ resummation contributions? Here we address this question. Clearly the specification of the non-perturbative input to the QCD evolution will be crucial.

Recall that the basic dynamical quantity at low x is the gluon distribution $f(x, k_T^2)$ un-integrated over its transverse momentum k_T . It is related to the conventional gluon density $g(x, Q^2)$ by

$$xg(x, Q^2) = \int^{Q^2} \frac{dk_T^2}{k_T^2} f(x, k_T^2). \quad (1)$$

In the leading $\ln(1/x)$ approximation $f(x, k_T^2)$ satisfies the BFKL equation and exhibits an $x^{-\omega_0}$ growth and a diffusion in $\ln k_T^2$ as $x \rightarrow 0$, where the BFKL or so-called hard Pomeron intercept $\omega_0 = (3\alpha_S/\pi)4 \ln 2$ for fixed α_S . The observable quantities are computed in terms of f via the k_T (or high energy) factorization prescription [8, 9]. For example, the structure functions F_i are given by

$$F_i = F_i^{\gamma g} \otimes f \quad (2)$$

where \otimes denotes a convolution in transverse, as well as longitudinal, momentum. Here $F_i^{\gamma g}$ are the off-shell gluon structure functions, which at lowest order are determined by the quark box (and crossed-box) contributions to photon-gluon fusion, see Fig. 1.

The BFKL gluon $f(x, k_T^2)$ and k_T (or high energy) factorization theorem were used [10] to predict the small x behaviour of F_2 prior to the measurements at HERA. The method used a starting distribution $f(x_0, k_T^2)$ at, say, $x_0 = 0.01$ deduced from an integrated gluon $g(x_0, Q^2)$ which had been determined in a global parton analysis of fixed-target deep inelastic and related scattering data. With this input the BFKL equation was solved to determine $f(x, k_T^2)$ in the small x domain ($x < x_0$). A major uncertainty in this procedure to predict F_2 is the treatment of the infrared region, $k_T^2 < k_0^2$. A recent study [11] using this approach finds that the BFKL predictions for F_2 increase too steeply with decreasing x in comparison with the HERA measurements, and concludes that there is no evidence for the effects of the resummation of $\ln(1/x)$ terms. Before we accept such a conclusion we should note the limitations of this form of the test of the BFKL k_T -factorization approach.

It is assumed [11, 12] that in the infrared region $f(x, k_T^2)$ has the form

$$f(x, k_T^2 < k_0^2) = \frac{k_T^2}{k_T^2 + k_a^2} \frac{k_0^2 + k_a^2}{k_0^2} f(x, k_0^2) \quad (3)$$

with $k_0^2 = 1 \text{ GeV}^2$ say, and where k_a^2 is an adjustable parameter. It turns out that there is a sizeable contribution from the infrared non-perturbative region which, since it is tied to $f(x, k_0^2)$, is forced to have the BFKL growth with decreasing x . The formalism does not include the GLAP leading $\ln Q^2$ resummations which go beyond the leading $\ln(1/x)$ approximation. Finally it should be noted that the BFKL equation for $f(x, k_T^2)$ only resums the leading order $\ln(1/x)$ terms. Sub-leading $\ln(1/x)$ effects are expected to reduce the growth of f with decreasing x .

Clearly this simplified procedure provides only a crude test of the underlying dynamics in the small x (HERA) domain. The main deficiencies are the treatment of the infrared region and the lack of a unified approach which incorporates both the BFKL $\ln(1/x)$ and the GLAP $\ln(Q^2)$ resummations. An important development is the demonstration by [8, 9, 10] that at the leading twist level the BFKL k_T factorization approach can be reduced to the conventional collinear GLAP factorization in which the anomalous dimensions and coefficient functions are extended to include the full resummation of leading $\ln(1/x)$ terms. This motivated an informative study by Thorne [13]. He has shown (in a scheme independent way) that the inclusion of the $\ln(1/x)$ terms within the collinear factorization approach gives a satisfactory, and even an improved, description of the F_2 data. He assumes non-perturbative components to the input distributions for the observables at scale Q_0^2 which are ‘flat’ at small x , and which are the *only* contributions at the scale ($A_{LL} \lesssim 1\text{GeV}^2$) that denotes the boundary between the perturbative and non-perturbative regions. In this way he demands that the rise of the structure functions with decreasing x must entirely come from perturbative effects. In summary Thorne finds, within the collinear factorization framework, that the ‘BFKL’ $\ln(1/x)$ terms are not excluded, but rather are favoured, by the F_2 data.

The agreement with the data obtained by Thorne [13] is contrary to the conclusion of ref. [11] which was based on the BFKL gluon and k_T factorization. This suggests that the application of the k_T factorization approach was too simplistic. Here we re-examine and improve the determination of $f(x, k_T^2)$ and, via k_T factorization, obtain a more realistic description of F_2 .

The first improvement is that we study a ‘unified’ equation for $f(x, k_T^2)$ which incorporates BFKL and GLAP evolution on an equal footing [14]. To be precise we solve a coupled pair of integral equations for the gluon and sea quark distributions, as well as allowing for the effects of the valence quarks. In this way we eliminate the problems of matching at $x = x_0$. A second improvement is a more physical treatment of the non-perturbative (or infrared) contributions to the BFKL equation and the k_T factorization integrals. We shall see that the former can be specified entirely by the *integrated* gluon distribution at the scale $Q^2 = k_0^2$ which marks the boundary of the perturbative and non-perturbative regions, whereas the integrals also need a non-perturbative component of the sea. In fact we find that an excellent description of the HERA measurements of F_2 is possible in terms of just two physically motivated parameters which fully determine these infrared contributions.

There is considerable merit in going back from the collinear to the k_T factorization approach for the description of small x deep inelastic scattering. Indeed, in the reduction to collinear form we lose some of the physical structure which is contained in the gluon ladder and k_T factorization. We discuss these limitations of the collinear approach below.

First we note that the high energy (or low x) behaviour of the structure functions is driven by the BFKL gluon ladder coupled (through k_T factorization) to the photon via the quark box. The corresponding Feynman diagram has a calculable perturbative contribution for all Q^2 (except for $Q^2 \rightarrow 0$ for massless quarks). The ‘hard’ or ‘QCD’ pomeron contribution generated by this ladder is thus present for all Q^2 . In particular there is a known perturbative contribution to the structure functions at $Q^2 = k_0^2$ coming from configurations in which the gluon transverse momenta within the ladder lie in the perturbative domain $k_T^2 > k_0^2$. This contrasts with the collinear factorization approach in which it is contrived to describe the observables in terms of a purely non-perturbative contribution at some scale, say $Q^2 = k_0^2$. The perturbative component, which must be present at $Q^2 = k_0^2$, will be evident in the k_T factorization approach that we introduce below.

A more subtle limitation of the Renormalisation Group (RG) and collinear factorization approach at small x concerns the treatment of the running of α_S . We solve the BFKL equation with running, rather than fixed, coupling where α_S depends on the local scale k_T^2 along the ladder. This way of implementing the running of α_S is supported by the calculation of next-to-leading $\ln(1/x)$ effects [15, 16]. The solution of the BFKL equation with running α_S can be reduced to the conventional RG form using saddle point techniques. However, the saddle point approximation is not applicable for arbitrarily small values of x [17, 3, 15, 16, 18, 19].

A third advantage of the k_T factorization approach is that it allows us to appropriately constrain the transverse momenta of the emitted gluons along the BFKL ladder. We are therefore able to quantify the effect of imposing this constraint. (Recall that in the usual application of the BFKL equation the gluon transverse momenta are taken to be unlimited.) We will see that the kinematic constraint largely subsumes the angular ordering constraint which is the basis of the ‘CCFM’ equation [20, 21]. The CCFM equation also incorporates both BFKL and GLAP evolution.

Another difference is that the BFKL contribution is a sum over all twists, whereas when it is reduced to collinear form only the leading twist is conventionally retained. Finally k_T factorization is much simpler to implement at small x than collinear factorization. We deal with dynamical quantities (namely the BFKL kernel and the structure function of the off-shell gluon) which can be calculated perturbatively. We calculate them to first order in α_S . Essentially the $\alpha_S \ln(1/x)$ terms are effectively resummed by simply integrating over the entire k_T^2 phase space allowed for the gluon ladder and the k_T factorization integrals.

In summary, the natural framework with which to describe observables at small x is the *unintegrated* gluon density $f(x, k_T^2)$ together with the *k_T factorization theorem*. (Here we use it to calculate the observable deep inelastic scattering structure functions F_2 and F_L .) That is, at small x the distribution $f(x, k_T^2)$ is the basic, universal quantity which can be taken from

process to process. If we were to reduce this framework to a collinear factorized form then the “simple”, but rich, physics structure of the gluon ladder is not fully taken into account and even may be distorted. It could be argued that most of the effects occur at subleading order in $\ln(1/x)$ and since only the leading order is completely known, little is lost. However, the effects have a direct physical origin. They are clearly present and are expected to be the dominant corrections in a more complete analysis.

Since we shall unify the BFKL and GLAP formalisms, the resulting equation for $f(x, k_T^2)$ is valid both for small x and large x . Moreover the region where the ‘BFKL’ $\ln(1/x)$ effects become significant will be decided by the underlying dynamics (QCD). We use the formalism to fit to deep inelastic data and so we are able to quantify the importance of BFKL effects.

The outline of the paper is as follows. In Section 2 we make modifications to the BFKL equation for the unintegrated gluon distribution $f(x, k^2)$ which allow for the GLAP leading $\ln Q^2$ contributions and which enable all the non-perturbative effects to be encapsulated in an input distribution for the integrated gluon, $xg(x, k_0^2)$. In Section 3 we introduce the equation for the quark singlet (momentum) distribution $\Sigma(x, Q^2)$, again paying particular attention to isolate the contribution to the non-perturbative region and to ensure that the perturbative terms are allowed to contribute for *all* Q^2 . In Section 4 we numerically solve the coupled integral equations for f and Σ . The k_T factorization theorem is used to calculate $F_2(x, Q^2)$ as a function of the two parameters that specify the input gluon (which we take to be ‘flat’ at small x). Optimum fits to the available F_2 data at small x are presented, and predictions are made for the charm component F_2^c and for the longitudinal structure function F_L . Finally, in Section 5 we present our conclusions.

2. Unified BFKL and GLAP equation for the gluon

We start from the BFKL equation for the unintegrated gluon distribution

$$f(x, k^2) = f^{(0)}(x, k^2) + \bar{\alpha}_S(k^2) k^2 \int_x^1 \frac{dz}{z} \int \frac{dk'^2}{k'^2} \left\{ \frac{f(x/z, k'^2) - f(x/z, k^2)}{|k'^2 - k^2|} + \frac{f(x/z, k^2)}{[4k'^4 + k^4]^{\frac{1}{2}}} \right\} \quad (4)$$

where $\bar{\alpha}_S = 3\alpha_S/\pi$ and $k \equiv k_T, k' \equiv k'_T$ denote the transverse momenta of the gluons, see Fig. 1. The equation corresponds to the leading $\ln(1/x)$ approximation.

2.1 From the BFKL to the unified equation

In order to make the BFKL equation for the gluon more realistic and to extend its validity to cover the full range of x we make the following modifications. First, to incorporate leading order GLAP evolution, we add on to the right-hand side of (4) the term [14]

$$\bar{\alpha}_S(k^2) \int_x^1 \frac{dz}{z} \left(\frac{z}{6} P_{gg}(z) - 1 \right) \frac{x}{z} g\left(\frac{x}{z}, k^2\right)$$

(5)

$$\equiv \bar{\alpha}_S(k^2) \int_x^1 \frac{dz}{z} \left(\frac{z}{6} P_{gg}(z) - 1 \right) \left\{ \frac{x}{z} g\left(\frac{x}{z}, k_0^2\right) + \int_{k_0^2}^{k^2} \frac{dk'^2}{k'^2} f\left(\frac{x}{z}, k'^2\right) \right\},$$

where we have used (1). The -1 allows for the contribution which is already included in the BFKL equation. The inclusion of the additional term (5) gives contributions to the gluon anomalous dimension γ_{gg} which are subleading in $\alpha_S \ln(1/x)$ but leading in α_S . These standard leading order GLAP contributions have an impact on the gluon intercept. They soften the small x rise of the gluon distribution and also change its overall normalisation.

The second modification to (4) is the introduction of the kinematic constraint [22, 23]

$$k'^2 < k^2/z \tag{6}$$

on the real gluon emission term, that is, on the integral over $f(x/z, k'^2)$. The origin of the constraint is the requirement that the virtuality of the exchanged gluon is dominated by its transverse momentum, $|k'^2| \simeq k_T'^2$. For clarity we have restored the subscript T in this equation. The constraint is another physically motivated, subleading correction in $\alpha_S \ln(1/x)$.

Thirdly, we notice that the integration region over k'^2 in (4) extends down to $k'^2 = 0$ where we expect that non-perturbative effects will affect the behaviour of $f(x, k'^2)$. We are only going to solve equation (4) in the perturbative region, defined by $k^2 > k_0^2$, so we only have to worry about the infrared contribution due to the real emission term from the interval $0 < k'^2 < k_0^2$. We may rewrite this infrared contribution in the form

$$k^2 \int_0^{k_0^2} \frac{dk'^2}{k'^2 |k'^2 - k^2|} f\left(\frac{x}{z}, k'^2\right) \simeq \int_0^{k_0^2} \frac{dk'^2}{k'^2} f\left(\frac{x}{z}, k'^2\right) \equiv \frac{x}{z} g\left(\frac{x}{z}, k_0^2\right). \tag{7}$$

The parameter $k_0^2 (\equiv Q_0^2)$ denotes the border between the perturbative and non-perturbative regions. Its magnitude will be taken to be around 1GeV^2 .

Finally we must of course add to the right-hand side of (4) the term which allows the quarks to contribute to the evolution of the gluon, that is

$$\frac{\alpha_S(k^2)}{2\pi} \int_x^1 dz P_{gq}(z) \Sigma\left(\frac{x}{z}, k^2\right) \tag{8}$$

where Σ is the singlet quark momentum distribution. To be explicit

$$\begin{aligned} \Sigma(x, k^2) &= \sum_{q=u,d,s} x(q + \bar{q}) + x(c + \bar{c}) \\ &\equiv V(x, k^2) + S_{uds}(x, k^2) + S_c(x, k^2) \end{aligned} \tag{9}$$

where V , S_{uds} and S_c denote the valence, the light sea quark and the charm quark contributions respectively. We discuss the evolution equation for $\Sigma(x, k^2)$ in the next section.

Gathering together all the above modifications, equation (4) for the gluon becomes

$$\begin{aligned}
f(x, k^2) &= \tilde{f}^{(0)}(x, k^2) \\
&+ \bar{\alpha}_S(k^2) k^2 \int_x^1 \frac{dz}{z} \int_{k_0^2}^{k'^2} \frac{dk'^2}{k'^2} \left\{ \frac{f\left(\frac{x}{z}, k'^2\right) \Theta\left(\frac{k^2}{z} - k'^2\right) - f\left(\frac{x}{z}, k^2\right)}{|k'^2 - k^2|} + \frac{f\left(\frac{x}{z}, k^2\right)}{[4k'^4 + k^4]^{\frac{1}{2}}} \right\} \\
&+ \bar{\alpha}_S(k^2) \int_x^1 \frac{dz}{z} \left(\frac{z}{6} P_{gg}(z) - 1 \right) \int_{k_0^2}^{k^2} \frac{dk'^2}{k'^2} f\left(\frac{x}{z}, k'^2\right) + \frac{\alpha_S(k^2)}{2\pi} \int_x^1 dz P_{gq}(z) \Sigma\left(\frac{x}{z}, k^2\right),
\end{aligned} \tag{10}$$

where now the driving term has the form

$$\tilde{f}^{(0)}(x, k^2) = f^{(0)}(x, k^2) + \frac{\alpha_S(k^2)}{2\pi} \int_x^1 dz P_{gg}(z) \frac{x}{z} g\left(\frac{x}{z}, k_0^2\right). \tag{11}$$

In (10) we include the constraint $k'^2 > k_0^2$ on the virtual, as well as the real, contributions in order to avoid spurious singularities at $k^2 = k_0^2$. In the perturbative region, $k^2 > k_0^2$, we may safely neglect the genuinely non-perturbative contribution $f^{(0)}(x, k^2)$ which is expected to decrease strongly with increasing k^2 . It is important to note that we have avoided the necessity to parametrize $f(x, k^2)$ in the non-perturbative region. Equation (10) only involves $f(x, k^2)$ in the perturbative domain, $k^2 > k_0^2$. The input (11) is provided by the conventional gluon at the scale k_0^2 . That is the input to our ‘unified BFKL + GLAP’ equation is determined by the same distribution as in conventional GLAP evolution. The modifications to (4) allow us to overcome the serious limitations discussed in the introduction. Surprisingly, we find that we can achieve an excellent description of all the deep inelastic data using the most economical parametrization of the input gluon

$$xg(x, k_0^2) = N(1-x)^\beta.$$

In particular the observed growth in $F_2(x, Q^2)$ with decreasing x is generated entirely by *perturbative* ($\ln(1/x)$ and $\ln Q^2$) dynamics.

It is easy to see how eq. (10) reduces to the conventional GLAP evolution equation for the gluon in the leading $\ln Q^2$ (or rather $\ln k^2$) approximation. The leading $\ln k^2$ terms arise from the strongly ordered configuration, $k_0^2 \ll k'^2 \ll k^2$, for the real emission contributions and to the neglect of the virtual contributions. Then (10) becomes

$$\begin{aligned}
f(x, k^2) &= \frac{\alpha_S(k^2)}{2\pi} \int_x^1 dz P_{gg}(z) \left[\frac{x}{z} g\left(\frac{x}{z}, k_0^2\right) + \int_{k_0^2}^{k^2} \frac{dk'^2}{k'^2} f\left(\frac{x}{z}, k'^2\right) \right] \\
&+ \frac{\alpha_S(k^2)}{2\pi} \int_x^1 dz P_{gq}(z) \Sigma\left(\frac{x}{z}, k^2\right),
\end{aligned} \tag{12}$$

where we have taken into account (11) and the remarks concerning the omission of $f^{(0)}$. Upon using (1) we see that (12) becomes

$$\frac{\partial(xg(x, k^2))}{\partial \ln k^2} = \frac{\alpha_S(k^2)}{2\pi} \int_x^1 dz \left[P_{gg}(z) \frac{x}{z} g\left(\frac{x}{z}, k^2\right) + P_{gq}(z) \Sigma\left(\frac{x}{z}, k^2\right) \right], \quad (13)$$

which is simply the GLAP evolution equation for the gluon.

2.2 Anomalous dimension of the gluon.

We will solve (10) for the unintegrated gluon. However first we anticipate the general behaviour of the anomalous dimension of the gluon which will come from this equation. To do this we rewrite the equation in terms of the moment function

$$\bar{f}(\omega, k^2) = \int_0^1 dx x^{\omega-1} f(x, k^2). \quad (14)$$

We have

$$\begin{aligned} \bar{f}(\omega, k^2) &= \bar{f}^{(0)}(\omega, k^2) + \frac{\bar{\alpha}_S(k^2)}{\omega} k^2 \int_{k_0^2}^{\infty} \frac{dk'^2}{k'^2} \\ &\left\{ \frac{\bar{f}(\omega, k'^2) \left[\Theta(k^2 - k'^2) + (k^2/k'^2)^\omega \Theta(k'^2 - k^2) \right] - \bar{f}(\omega, k^2)}{|k'^2 - k^2|} + \frac{\bar{f}(\omega, k^2)}{(4k'^4 + k^4)^{\frac{1}{2}}} \right\} \\ &+ \bar{\alpha}_S(k^2) P(\omega) \int_{k_0^2}^{k^2} \frac{dk'^2}{k'^2} \bar{f}(\omega, k'^2) \end{aligned} \quad (15)$$

where we have neglected, for simplicity, the contribution coming from the quarks and where $P(\omega)$ is the moment function of $(zP_{gg}(z)/6 - 1)$. The term in square brackets is due to the kinematic constraint. Without this constraint we would have 1 instead of $(k^2/k'^2)^\omega$, and the two Θ functions would simply sum to unity.

For large k^2 the moment function behaves as

$$\bar{f}(\omega, k^2) \sim \left(\frac{k^2}{k_0^2} \right)^{\gamma_{gg}(\omega, \bar{\alpha}_S)} \quad (16)$$

where, for illustration, we take fixed α_S . The quantity γ_{gg} is the anomalous dimension of the gluon. If we insert (16) into (15) then we find, after some algebra, the following implicit equation for γ_{gg}

$$1 - \frac{\bar{\alpha}_S}{\omega} K(\gamma_{gg}, \omega) - \frac{\bar{\alpha}_S}{\gamma_{gg}} P(\omega) = 0 \quad (17)$$

where K , the double moment of the kernel in (15), is given by

$$K(\gamma, \omega) = \int_0^\infty \frac{d\rho}{\rho} \left\{ \frac{[\rho^\gamma \Theta(1 - \rho) + \rho^{\gamma-\omega} \Theta(\rho - 1)] - 1}{|\rho - 1|} + \frac{1}{[4\rho^2 + 1]^{\frac{1}{2}}} \right\}. \quad (18)$$

If $\omega = 0$ then the expression in square brackets reduce to ρ^γ and we have the familiar BKFL result

$$K(\gamma, \omega = 0) = [2\Psi(1) - \Psi(\gamma) - \Psi(1 - \gamma)] \quad (19)$$

where Ψ is the logarithmic derivative of the Euler gamma function.

It is clear that γ_{gg} , which satisfies (17), is of the form¹

$$\gamma_{gg}(\omega, \bar{\alpha}_S) = \gamma^{\text{BFKL}}\left(\frac{\bar{\alpha}_S}{\omega}\right) + \bar{\alpha}_S P(\omega) + \text{higher order terms}, \quad (20)$$

where γ^{BFKL} satisfies the usual equation

$$1 - \frac{\bar{\alpha}_S}{\omega} K(\gamma^{\text{BFKL}}, \omega = 0) = 0. \quad (21)$$

The higher order terms include contributions which are subleading in $\bar{\alpha}_S/\omega$ as well as in $\bar{\alpha}_S$. The anomalous dimension γ_{gg} has a branch point singularity in the ω plane, whose position $\omega = \omega_0(\bar{\alpha}_S)$ controls the small x behaviour of the gluon distribution. The inverse of (14) gives

$$f(x, k^2) \sim x^{-\omega_0(\bar{\alpha}_S)}. \quad (22)$$

The value of ω_0 is obtained from the requirement that

$$\frac{\partial}{\partial \gamma} \left\{ 1 - \frac{\bar{\alpha}_S}{\omega_0} K(\gamma, \omega_0) - \frac{\bar{\alpha}_S}{\gamma} P(\omega_0) \right\} = 0, \quad (23)$$

together with the equation

$$1 - \frac{\bar{\alpha}_S}{\omega_0} K(\gamma, \omega_0) - \frac{\bar{\alpha}_S}{\gamma} P(\omega_0) = 0, \quad (24)$$

see (17). Recall that in the leading $\ln(1/x)$ (or leading $1/\omega$) approximation (23) reduces to

$$\partial K(\gamma, 0) / \partial \gamma = 0, \quad (25)$$

which is satisfied when $\gamma = \frac{1}{2}$. Thus from (21) we obtain the well-known BFKL result that

$$\omega_0 = \bar{\alpha}_S K(\gamma = \frac{1}{2}, \omega = 0) = \bar{\alpha}_S 4 \ln 2. \quad (26)$$

The relevant domain for solving the pair of equations (17) and (21) is $0 < \gamma < 1$ and $\omega > 0$. In this region the Mellin transform of the non-singular part of the gluon splitting function satisfies

$$P(\omega) < 0, \quad (27)$$

and moreover

$$K(\gamma, \omega) < K(\gamma, 0). \quad (28)$$

¹If we were to replace γ^{BFKL} simply by the term which is leading order in α_S , that is $\bar{\alpha}_S/\omega$, then the sum of the first two terms of (20) gives the conventional GLAP anomalous dimension.

Thus both the additional non-singular part of the GLAP splitting function ($P_{gg} - 6/z$) and the kinematic constraint (which takes $K(\gamma, 0)$ to $K(\gamma, \omega)$) tend to reduce the magnitude of ω_0 from the BFKL value shown in (26). These corrections are of course subleading in $\ln(1/x)$. Our numerical analysis with running α_S reflects this softening of the $x^{-\omega_0}$ singular behaviour.

2.3 The CCFM equation

A more general treatment of the gluon ladder, which follows from the BKFL formalism is provided by the Catani-Ciafaloni-Fiorani-Marchesini (CCFM) equation based on angular ordering of the gluon emission along the chain [20, 21, 24]. The equation embodies both the BKFL equation at small x and the conventional GLAP evolution at large x . The unintegrated gluon distribution f now acquires a dependence on an additional scale (which we may take to be Q^2) that specifies the maximal angle of gluon emission. The CCFM equation has the form

$$f(x, k^2, Q^2) = f^{(0)}(x, k^2, Q^2) + \bar{\alpha}_S \int_x^1 \frac{dz}{z} \int \frac{d^2q}{\pi q^2} \Theta(Q - qz) \Delta_R(z, k^2, q^2) \frac{k^2}{(\mathbf{q} + \mathbf{k})^2} f\left(\frac{x}{z}, (\mathbf{q} + \mathbf{k})^2, q^2\right) \quad (29)$$

where the theta function $\Theta(Q - qz)$ reflects the angular ordering constraint on the emitted gluon. The so-called ‘non-Sudakov’ form-factor Δ_R is given by

$$\Delta_R(z, k^2, q^2) = \exp \left[-\bar{\alpha}_S \int_z^1 \frac{dz'}{z'} \int \frac{dq'^2}{q'^2} \Theta(q' - z'q) \Theta(k^2 - q'^2) \right]. \quad (30)$$

Eq. (29) contains only the singular $1/z$ term of the $g \rightarrow gg$ splitting function (which is screened by the virtual corrections contained in Δ_R). Its generalisation to include the remaining parts of this vertex (as well as the quark contributions) is possible. Eq. (29) has been solved numerically in the small x domain and the solution for $f(x, k^2, Q^2)$ was presented in [21]. The CCFM equation, which is a generalisation of the BFKL equation, generates a steep $x^{-\omega_0}$ type of behaviour² but ω_0 now acquires significant subleading $\ln(1/x)$ corrections which come from the angular ordering constraint [26]. The constraint also introduces subleading terms in the anomalous dimension

$$\gamma_{gg} = \gamma_{gg}^{\text{BFKL}} \left(\frac{\bar{\alpha}_S}{\omega} \right) + \bar{\alpha}_S h \left(\frac{\bar{\alpha}_S}{\omega} \right) + \dots$$

so the angular ordering constraint which gives rise to the CCFM equation and the kinematic constraint (7) lead to similar effects – both give subleading $\ln(1/x)$ corrections to the ‘‘QCD Pomeron intercept’’ ω_0 and to the gluon anomalous dimension γ_{gg} . We found that the kinematic constraint overrides the angular ordering constraint except possibly in the large x domain when $Q^2 < k^2$ [22], see also [23]. Thus in our formulation we neglect the angular ordering constraint altogether.

3. The equation for the quark distribution

²The effect on F_2 is considered in [25].

At small x the gluon drives the sea quark (momentum) distribution S via the $g \rightarrow q\bar{q}$ transition, see Fig. 1. We evaluate the effect using the k_T factorization theorem. To be precise we use the k_T factorization prescription to calculate observables (such as F_2) directly from the unintegrated gluon distribution $f(x, k_T^2)$. For F_2 we interpret the result in terms of the sea quark distributions, implicitly assuming the DIS scheme. The total sea is the sum of the individual quark contributions

$$S(x, Q^2) = \sum_q S_q(x, Q^2).$$

At small x the factorization theorem gives

$$S_q(x, Q^2) = \int_x^1 \frac{dz}{z} \int \frac{dk^2}{k^2} S_{\text{box}}^q(z, k^2, Q^2) f\left(\frac{x}{z}, k^2\right) \quad (31)$$

where S_{box} describes the quark box (and crossed box) contribution shown in Fig. 1. S_{box} implicitly includes an integration over the transverse momentum, κ , of the exchanged quark. Indeed, evaluating the box contributions we find

$$\begin{aligned} S_q(x, Q^2) &= \frac{Q^2}{4\pi^2} \int \frac{dk^2}{k^4} \int_0^1 d\beta \int d^2\kappa' \alpha_S \left\{ [\beta^2 + (1-\beta)^2] \left(\frac{\kappa}{D_{1q}} - \frac{\kappa - \mathbf{k}}{D_{2q}} \right)^2 \right. \\ &\quad \left. + [m_q^2 + 4Q^2\beta^2(1-\beta)^2] \left(\frac{1}{D_{1q}} - \frac{1}{D_{2q}} \right)^2 \right\} f\left(\frac{x}{z}, k^2\right) \Theta\left(1 - \frac{x}{z}\right) \quad (32) \end{aligned}$$

where $\kappa' = \kappa - (1-\beta)k$ and

$$\begin{aligned} D_{1q} &= \kappa^2 + \beta(1-\beta)Q^2 + m_q^2 \\ D_{2q} &= (\kappa - \mathbf{k})^2 + \beta(1-\beta)Q^2 + m_q^2 \\ z &= \left[1 + \frac{\kappa'^2 + m_q^2}{\beta(1-\beta)Q^2} + \frac{k^2}{Q^2} \right]^{-1}. \quad (33) \end{aligned}$$

The argument of α_S is taken as $(k^2 + \kappa'^2) + m_q^2$. We set the quark masses to be $m_u = m_d = m_s = 0$ and $m_c = 1.4$ GeV.

3.1 The light quark component of the sea

We first discuss the calculation of the contribution of the “massless” u, d, s quarks to the total sea distribution S . It is necessary to consider three different regions of the k and κ' integrations of (32).

- (a) The contribution from the non-perturbative region $k^2, \kappa'^2 < k_0^2$ is evaluated phenomenologically assuming that it is dominated by “soft” Pomeron exchange [27]. The contribution is parametrized by the form

$$S^{(a)} = S_u^P + S_d^P + S_s^P \quad (34)$$

where

$$S_u^{\mathbb{P}} = S_d^{\mathbb{P}} = 2S_s^{\mathbb{P}} = C_{\mathbb{P}} x^{-0.08} (1-x)^8. \quad (35)$$

The coefficient $C_{\mathbb{P}}$ is independent of Q^2 (in the large Q^2 region) since the contribution arises from the region in which the struck quarks have limited transverse momentum, $\kappa^2 < k_0^2$.

- (b) In the region $k^2 < k_0^2 < \kappa'^2$ we apply the strong-ordered approximation at the quark-gluon vertex and take [28]

$$S_{\text{box}} \rightarrow S_{\text{box}}^{(b)}(z, k^2 = 0, Q^2). \quad (36)$$

Then the contribution to (31) from this domain becomes

$$\begin{aligned} S^{(b)} &= \int_x^1 \frac{dz}{z} S_{\text{box}}^{(b)}(z, k^2 = 0, Q^2) \int_0^{k_0^2} \frac{dk^2}{k^2} f\left(\frac{x}{z}, k^2\right) \\ &= \int_x^1 \frac{dz}{z} S_{\text{box}}^{(b)}(z, k^2 = 0, Q^2) \frac{x}{z} g\left(\frac{x}{z}, k_0^2\right) \end{aligned} \quad (37)$$

where the summation over u, d, s is implicitly assumed. The potential collinear singularities in the on-shell structure function S_{box} are regulated by the cut-off k_0^2 . Recall that $\kappa^2 \simeq \kappa'^2 > k_0^2$.

- (c) In the remaining region, $k^2 > k_0^2$, eq. (32) is left unchanged. To be precise we use the perturbative expression for $S_q(x, Q^2)$.

3.2 The charm component

The calculation of the charm component of the sea follows perturbative QCD in all regions. To evaluate $S_{q=c}$ we divide the integration over k^2 into the regions $k^2 < k_0^2$ and $k^2 > k_0^2$. For $k^2 < k_0^2$, which we denote region (b), we use the on-shell approximation to evaluate S_{box} . That is we calculate $S_{\text{box}}(z, k^2 = 0, Q^2; m_c^2)$, which is finite due to $m_c \neq 0$. Then (31) gives

$$S_{q=c}^{(b)}(x, Q^2) = \int_x^a \frac{dz}{z} S_{\text{box}}(z, k^2 = 0, Q^2; m_c^2) \int_0^{k_0^2} \frac{dk^2}{k^2} f\left(\frac{x}{z}, k^2\right) \quad (38)$$

where $a = (1 + 4m_c^2/Q^2)^{-1}$, see (33). For $k^2 > k_0^2$, which we call region (c), we use the full perturbative formula. Thus adding the two contributions we have

$$\begin{aligned} S_{q=c}(x, Q^2) &= \int_x^a \frac{dz}{z} S_{\text{box}}(z, k^2 = 0, Q^2; m_c^2) \frac{x}{z} g\left(\frac{x}{z}, k_0^2\right) \\ &\quad + \int_x^a \frac{dz}{z} \int_{k_0^2} \frac{dk^2}{k^2} S_{\text{box}}(z, k^2, Q^2; m_c^2) f\left(\frac{x}{z}, k^2\right), \end{aligned} \quad (39)$$

where we have used (1) which enables $S_{q=c}$ is to be specified in terms of the conventional gluon input distribution.

3.3 The equation for the quark singlet distribution

Besides S , the singlet momentum distribution Σ also contains a valence quark contribution V , which is taken from a known set of partons. Thus in summary the singlet distribution is

$$\Sigma = (S^{(a)} + S^{(b)} + S^{(c)})_{uds} + (S^{(b)} + S^{(c)})_{q=c} + V, \quad (40)$$

where $S^{(a)}$ is phenomenologically parametrized in terms of “soft” Pomeron exchange and the $S^{(b)}$ terms are determined perturbatively except for the (non-perturbative) input gluon distribution at scale k_0^2 . The $S^{(c)}$ terms are defined entirely in terms of the unintegrated gluon distribution f in the perturbative region $k^2 > k_0^2$. Finally, $V = x(u_{\text{val}} + d_{\text{val}})$ is the valence quark contribution.

In order to see the connection with the GLAP evolution of the (light) quark sea we first note that

$$S_q(x, Q^2) = S_q(x, k_0^2) + \int_{k_0^2}^{Q^2} \frac{\partial S_q(x, Q'^2)}{\partial Q'^2} dQ'^2, \quad (41)$$

where here S denotes the sum over just the u , d and s quarks. We next recall that the leading twist part of the k_T factorization formula (31), written in the form

$$Q^2 \frac{\partial S_q(x, Q^2)}{\partial Q^2} = \int_x^1 \frac{dz}{z} \int \frac{dk^2}{k^2} Q^2 \frac{\partial S_{\text{box}}^q(z, k^2, Q^2)}{\partial Q^2} f\left(\frac{x}{z}, k^2\right), \quad (42)$$

can be reduced to the collinear form [18]

$$Q^2 \frac{\partial S_q(x, Q^2)}{\partial Q^2} = \frac{\alpha_S(Q^2)}{2\pi} \int_x^1 dz P_{qg}(z, \alpha_S(Q^2)) \frac{x}{z} g\left(\frac{x}{z}, Q^2\right) \quad (43)$$

which incorporates leading $\ln 1/x$ resummation effects in both the splitting function P_{qg} and in the integrated gluon distribution g . Thus (41) may be written in the form

$$S_q(x, Q^2) = S_q(x, k_0^2) + \int_{k_0^2}^{Q^2} \frac{dQ'^2}{Q'^2} \frac{\alpha_S(Q'^2)}{2\pi} \int_x^1 dz \left[P_{qg}(z, \alpha_S(Q'^2)) \frac{x}{z} g\left(\frac{x}{z}, Q'^2\right) + P_{qq}(z, \alpha_S(Q'^2)) S_q\left(\frac{x}{z}, Q'^2\right) \right], \quad (44)$$

where for consistency we have included the $S \rightarrow S$ contribution to the evolution. This additional term is needed to ensure the correct GLAP structure. Of course, at small x we expect S to be dominantly driven by the gluon. Equation (44) is simply the integral form of the GLAP evolution equation for the (light) sea quark (momentum) distribution, S .

Guided by the GLAP structure, it is clear that we should also add the $S \rightarrow S$ contribution to the complete equation (40) based on k_T factorization. Then (40) becomes

$$\begin{aligned} \Sigma(x, k^2) &= S^{(a)}(x) + \sum_q \int_x^a \frac{dz}{z} S_{\text{box}}^q(z, k'^2 = 0, k^2; m_q^2) \frac{x}{z} g\left(\frac{x}{z}, k_0^2\right) + V(x, k^2) \\ &+ \sum_q \int_{k_0^2}^{\infty} \frac{dk'^2}{k'^2} \int_x^1 \frac{dz}{z} S_{\text{box}}^q(z, k'^2, k^2; m_q^2) f\left(\frac{x}{z}, k'^2\right) \\ &+ \int_{k_0^2}^{k^2} \frac{dk'^2}{k'^2} \frac{\alpha_S(k'^2)}{2\pi} \int_x^1 dz P_{qq}(z) S_{uds}\left(\frac{x}{z}, k'^2\right) \end{aligned} \quad (45)$$

where $S^{(a)}$ is given by (34) and where the uds subscript indicates that the additional $S \rightarrow S$ term is only included for the light quarks. This equation for the singlet quark distribution Σ , together with eq. (10) for the gluon, form the pair of coupled equations which we solve. In this way we can specify the structure function F_2 in terms of the parameters of the input distributions, and hence determine the values of the parameters by fitting to the data for F_2 , see sections 4-6.

3.4 k_T versus collinear factorization and P_{qg}

As we have already mentioned, the *leading-twist* part of the k_T factorization formula can be rewritten in a collinear factorization form. Once the unintegrated gluon distribution is taken as a solution of the BFKL equation and the k_T factorization integral is performed over the *entire* available phase-space (i.e. not only over the region corresponding to the strongly ordered transverse momenta) then the leading small x effects are automatically resummed in the splitting functions and in the coefficient functions. The k_T factorization theorem can in fact be used as the tool for calculating these quantities [8, 9].

We illustrate this point by using the example of the calculation of the splitting function P_{qg} . For simplicity we assume that the coupling α_S is fixed and that the quarks are massless. We begin from the k_T factorization formula (42) written in moment space

$$Q^2 \frac{\partial \bar{S}(\omega, Q^2)}{\partial Q^2} = \int \frac{dk^2}{k^2} Q^2 \frac{\partial \bar{S}_{\text{box}}(\omega, Q^2/k^2)}{\partial Q^2} \bar{f}(\omega, k^2). \quad (46)$$

where we have noted, for massless quarks, that \bar{S}_{box} is a function of the ratio Q^2/k^2 . Thus we may factorise the convolution over k^2 by taking moments. We find

$$Q^2 \frac{\partial \bar{S}(\omega, Q^2)}{\partial Q^2} = \frac{1}{2\pi i} \int_{1/2-i\infty}^{1/2+i\infty} d\gamma \gamma \tilde{S}_{\text{box}}(\omega, \gamma) \tilde{f}(\omega, \gamma) \left(\frac{Q^2}{k_0^2} \right)^\gamma \quad (47)$$

where $\tilde{S}_q^{box}(\omega, \gamma)$ and $\tilde{f}(\omega, \gamma)$ are the Mellin transform of the moment functions $\bar{S}_q^{box}(\omega, k^2, Q^2)$ and $\bar{f}(\omega, k^2)$ i.e.

$$\bar{S}_{\text{box}}(\omega, k^2, Q^2) = \frac{1}{2\pi i} \int_{1/2-i\infty}^{1/2+i\infty} d\gamma \tilde{S}_{\text{box}}(\omega, \gamma) \left(\frac{Q^2}{k^2} \right)^\gamma \quad (48)$$

and

$$\bar{f}(\omega, k^2) = \frac{1}{2\pi i} \int_{1/2-i\infty}^{1/2+i\infty} d\gamma \tilde{f}(\omega, \gamma) \left(\frac{k^2}{k_0^2} \right)^\gamma. \quad (49)$$

Retaining the leading pole γ_{gg} contribution of $\tilde{f}(\omega, \gamma)$ in the γ plane, the integrals (47) and (49) can be evaluated to give

$$Q^2 \frac{\partial \bar{S}(\omega, Q^2)}{\partial Q^2} = \gamma_{gg}^2 \tilde{S}_{\text{box}}(\omega, \gamma_{gg}) C(\omega, \alpha_S) \left(\frac{Q^2}{k_0^2} \right)^{\gamma_{gg}} \quad (50)$$

and

$$\bar{f}(\omega, k^2) = \gamma_{gg} C(\omega, \alpha_S) \left(\frac{k^2}{k_0^2} \right)^{\gamma_{gg}}. \quad (51)$$

where $\gamma_{gg}C$ is the residue of the pole. The function $\gamma_{gg}(\bar{\alpha}_S, \omega)$ is the (leading twist) gluon anomalous dimension. From (51) we see that the integrated gluon is given by

$$\bar{g}(\omega, Q^2) = C(\omega, \alpha_S) \left(\frac{Q^2}{k_0^2} \right)^{\gamma_{gg}} \quad (52)$$

where $\bar{g}(\omega, Q^2)$ is the moment function of the (leading twist part) of the gluon distribution. Thus by comparing (50) with the conventional GLAP form

$$Q^2 \frac{\partial \bar{S}_q(\omega, Q^2)}{\partial Q^2} = \frac{\alpha_S}{2\pi} \bar{P}_{qg}(\omega, \alpha_S) \bar{g}(\omega, Q^2) \quad (53)$$

we can identify the moment of the P_{qg} splitting function to be

$$\frac{\alpha_S}{2\pi} \bar{P}_{qg}(\omega, \alpha_S) = \gamma_{gg}^2(\bar{\alpha}_S, \omega) \tilde{S}_{\text{box}}^q(\omega, \gamma_{gg}(\bar{\alpha}_S, \omega)) \quad (54)$$

in the so-called Q_0^2 regularization and DIS scheme [9] which we implicitly adopt.

In the leading $\ln(1/x)$ approximation we have

$$\frac{\alpha_S}{2\pi} \bar{P}_{qg}(\omega, \alpha_S) = (\gamma^{\text{BFKL}})^2 \tilde{S}_{\text{box}}^q(\omega = 0, \gamma^{\text{BFKL}}). \quad (55)$$

The anomalous dimension γ^{BFKL} has the following expansion [29]

$$\gamma^{\text{BFKL}}\left(\frac{\bar{\alpha}_S}{\omega}\right) = \sum_{n=1}^{\infty} c_n \left(\frac{\bar{\alpha}_S}{\omega}\right)^n \quad (56)$$

which in turn gives for the splitting function P_{qg}

$$zP_{qg}(z, \alpha_S) = \sum_{n=1}^{\infty} c_n \frac{[\bar{\alpha}_S \ln(1/z)]^{n-1}}{(n-1)!}, \quad (57)$$

whereas representation (55) generates the following

expansion of the splitting function $P_{qg}(z, \alpha_S)$ at small z

$$zP_{qg}(z, \alpha_S) = zP_{qg}^{(0)}(z) + \bar{\alpha}_s \sum_{n=1}^{\infty} b_n \frac{[\bar{\alpha}_S \ln(1/z)]^{n-1}}{(n-1)!}. \quad (58)$$

The first term on the right hand side vanishes at $z = 0$. It should be noted that the splitting function P_{qg} is formally non-leading at small z when compared with the splitting function P_{gg} . For moderately small values of z however, when the first few terms in the expansions (58) and (57) dominate, the BFKL effects can be much more important in P_{qg} than in P_{gg} .

This comes from the fact that all coefficients b_n in (58) are different from zero, while in (57) we have $c_2 = c_3 = 0$ [29]. The small x resummation effects within the conventional QCD evolution formalism have recently been discussed in refs. [30, 31, 32, 33, 34]. These studies already emphasize this point, namely that at the moderately small values of x which

are relevant for the HERA measurements, the $\ln(1/x)$ resummation effects in the splitting function P_{qg} have a much stronger impact on F_2 than do those in the splitting function P_{gg} . In particular we should also recall that the BFKL effects in the splitting function P_{qg} can significantly affect the extraction of the gluon distribution from the experimental data on the slope of the structure function F_2

$$Q^2 \frac{\partial F_2(x, Q^2)}{\partial Q^2} \simeq \sum_q e_q^2 \frac{\alpha_S(Q^2)}{2\pi} \int_x^1 dz P_{qg}(z, \alpha_S(Q^2)) \frac{x}{z} g\left(\frac{x}{z}, Q^2\right). \quad (59)$$

Here we also include the subleading $\ln(1/x)$ terms which would come from the subleading terms in γ_{gg} etc. Keeping the exact k_T factorisation (and not just its large Q^2 limit) we also include the non-leading twist contributions to F_2 . They would formally be generated by the contributions given by the (non-leading) twist anomalous dimensions.

4. Numerical analysis and the description of F_2

We now have a closed system of two coupled integral equations for two unknowns. Namely equation (10) of Section 2 for the unintegrated gluon distribution $f(x, k^2)$ and equation (45) of Section 3 for the integrated quark singlet (momentum) distribution $\Sigma(x, k^2)$. The effect of the gluon in the perturbative region, $k^2 > k_0^2$, is of special interest. It is the ‘dynamo’ which drives small x physics.

The advantage of this formulation of the unified BFKL/GLAP equation is that the input is well-controlled. We emphasized in Section 2 that the equation for $f(x, k^2)$ required only the specification of an input form for the integrated gluon,

$$xg(x, k_0^2) = N(1-x)^\beta, \quad (60)$$

say. Moreover, the equation for the singlet $\Sigma(x, k^2)$ requires as input only the non-perturbative sea contribution whose form we assume is given by the ‘soft’ Pomeron

$$S^{(a)} = C_P x^{-0.08} (1-x)^8 \quad (61)$$

and the contributions $S^{(b)}$ of (37) and (38) which depend on $xg(x, k_0^2)$ of (60). The choice of the exponent -0.08 is motivated by the Regge pomeron intercept found in the analysis of total cross section data [27]. We choose the exponent of $(1-x)$ to be 8, typical of the behaviour of the sea distribution. In our small x analysis any similar choice would be equally good and would not change the quality of the description.

The valence quark contribution $V(x, k^2)$ in (45), which is determined mainly by fixed target deep inelastic data, is taken from the leading order GRV set of partons [6]. We are therefore able to self-consistently determine $f(x, k^2)$ and $\Sigma(x, k^2)$ as functions of a small number of physically motivated parameters. In fact, we have only the two parameters, namely N and β determining the input gluon distribution (60). The momentum sum rule fixes the value of C_P , which determines the input sea, (61). The presence of BFKL - like terms means that the

momentum sum rule is not exactly conserved. However the violation is small. For example, after evolution to $Q^2 = 50\text{GeV}^2$ we find that the sum of the momentum fractions carried by the gluon and the light quarks is only increased from 1 to 1.007. We neglect this small violation of momentum conservation.

4.1 The optimum description of the F_2 data at small x

We determine the values of the input parameters by fitting to the HERA measurements of the proton structure function F_2 using

$$F_2 = \sum_q e_q^2(S_q + V_q), \quad (62)$$

which holds in the DIS scheme. We thus have to calculate $S_q(x, Q^2)$ in terms of the input gluon parameters N and β . To do this we solve the pair of equations (10) and (45) for $f(x, k^2)$ and $\Sigma(x, k^2)$ using an extension of the method proposed in [35]. This method incorporates the interpolation in two variables x and Q^2 with orthogonal polynomials. Thus the coupled integral equations can be transformed into the set of linear algebraic equations and readily solved. In this way we can express $F_2(x, Q^2)$ in terms of N and β . We then determine the optimum values of these parameters by fitting to the HERA [1] and fixed-target [36] data for $F_2(x, Q^2)$ that are available in the small x domain, $x < 0.1$. We take a running coupling which satisfies $\alpha_S(M_Z^2) = 0.12$.

We actually show the results of two fits. The first is the ‘realistic’ fit with the kinematic constraint imposed (which requires the virtuality of the exchanged gluons along the ladder to satisfy $|k'^2| \simeq k_T'^2$). Then for comparison we repeat the analysis without imposing the kinematic constraint, that is we omit Θ function in (10). The quality of the fits are shown in Figs. 2 and 3, and the parameters given in Table 1. To be precise Figs. 2 and 3 respectively show the description of the H1 and ZEUS data [1] together with those fixed-target data that occur at the same values of Q^2 .

The fit with the kinematic constraint included (continuous curves) is significantly better than that in which it is omitted (shown by the dashed curves). Without the constraint the predicted rise of F_2 is a little too steep at the smallest values of x and Q^2 . Over the remainder of the x, Q^2 domain the fit (fit 2) gives a good description of F_2 . It is far better, for example, than that shown in ref. [11].

The kinematic constraint, which corresponds to subleading $\ln(1/x)$ corrections, lowers the ‘hard’ pomeron intercept and improves the description of the data, particularly at the smaller values of x . In fact the resulting description of $F_2(x, Q^2)$ with just two free parameters (N and β) is excellent, and is comparable, even a little better than, to that achieved in the global parton analyses, see, for example, the χ^2 listed in Table 1. Moreover, the overall behaviour of the gluon is much more realistic than that of the fit without the kinematic constraint. It gives an acceptable description of the WA70 prompt photon data [37], which directly sample the gluon at $x \simeq 0.4$. These data were not used to constrain the gluon. For fit 1 the prediction is

some 30% above WA70 data, which is within the QCD scale uncertainties, whereas the gluon of fit 2 gives a prediction which is a factor of about 2.5 above the data. It is not surprising that the gluons are so different in the two fits since they are both contrived to give satisfactory description of the measurements of F_2 at small x , despite the fact that the kinematic constraint significantly reduces the gluon intercept ω_0 . It is encouraging that it is the description with the kinematic constraint that gives the acceptable large x behaviour of the gluon. For completeness we use our determination of the unintegrated gluon to compute the conventional gluon distribution $xg(x, Q^2)$ and compare the result with the gluons of recent sets of partons obtained in GLAP-based global analyses of deep inelastic and related data. To be specific the continuous curves in Fig. 4 compare the gluon calculated from $f(x, k_T^2)$ of the fit 1 (via eq. (1)) with the gluon distributions of the MRS(R2) [4] and GRV [6] set of partons (shown by the dashed and dotted curves respectively). We see that the behaviour of the integrated gluon is very similar to that of MRS(R2). This may be expected since the MRS analysis used to the same HERA data as those fitted in the present work, whereas these data were not available at the time of the GRV analysis. However, we emphasize the different underlying structure of the present analysis and the pure GLAP-based descriptions. We shall see below that in the unified BFKL/GLAP approach the rise of F_2 is generated essentially by $\ln(1/x)$ effects in the off-shell gluon structure, $F_2^{\gamma g}$ of Fig. 1.

	Kinematic constant	$xg = N(1-x)^\beta$		C_P	$\chi^2/\text{datapoint}$ [393 points]
		N	β		
Fit 1	yes	1.57	2.5	0.269	1.07
Fit 2	no	0.85	0.9	0.269	1.8
MRS(R2)					1.12

Table 1: The parameters N and β determined in the optimum fit to the available data [1, 36] for F_2 with $x < 0.05$ and $Q^2 > 1.5\text{GeV}^2$, without and with the inclusion of the kinematic constraint along the gluon ladder. The value of C_P of (35) is also shown, although this is fixed in terms of N and β by the momentum sum rule. For comparison we also show the χ^2 for the same set of HERA and fixed-target data obtained in a recent next-to-leading order GLAP global parton analysis [4]. For both fit 1 and 2 the gluon carries 45% of the proton's momentum at the input scale $k_0^2 = 1\text{GeV}^2$.

4.2 The effect of the $\ln(1/x)$ resummation on the gluon

Fig. 5 shows the behaviour of the unintegrated gluon distribution $f(x, k^2)$ as a function of k^2 for $x = 10^{-3}$ and 10^{-4} . Three different determinations are shown, each of which start from the input

$$xg(x, k_0^2) = 1.57(1-x)^{2.5}$$

of fit 1 of Table 1. The continuous and dashed curves correspond, respectively, to the behaviour with and without the kinematic constraint. The dotted curve is obtained from a GLAP determination in which the BFKL kernel in (10) is replaced by the leading order P_{gg} function. That is (10) is replaced by

$$f(x, k^2) = \frac{\alpha_S(k^2)}{2\pi} \left[\int_x^1 dz P_{gg}(z) \frac{x}{z} g\left(\frac{x}{z}, k_0^2\right) + \int_x^1 dz P_{gg}(z) \int_{k_0^2}^{k^2} \frac{dk'^2}{k'^2} f\left(\frac{x}{z}, k'^2\right) + \int_x^1 dz P_{gq}(z) \Sigma\left(\frac{x}{z}, k^2\right) \right], \quad (63)$$

where P_{gg} has the usual form

$$P_{gg}(z) = 6 \left[\frac{1-z}{z} + z(1-z) + \frac{z}{(1-z)_+} + \frac{11}{12} \delta(1-z) \right] - \frac{N_f}{3} \delta(1-z). \quad (64)$$

The comparison of the dashed and dotted curves shows that the differences between the BFKL and GLAP approaches are not very big, even for the values of x as low as 10^{-3} . The differences become more obvious when one considers smaller values of x , around 10^{-4} . Even then the discrepancies are only visible at lower values of k^2 . This effect can be explained in terms of power series expansion in α_S/ω of the gluon anomalous dimension

$$\gamma^{\text{BFKL}} = \frac{\bar{\alpha}_S}{\omega} + c_4 \left(\frac{\bar{\alpha}_S}{\omega} \right)^4 + \dots$$

see (56), where $c_2 = c_3 = c_5 = 0$. The first term of the expansion, which is common to BFKL and GLAP, is clearly dominant for the smaller values of $\alpha_S(k^2)$. Thus we confirm the well known result that, in the region of moderately small values of x relevant for the HERA measurements, $\ln(1/x)$ resummation has little effect on the gluon distribution. If the gluon input were adjusted to correspond to the optimum fit with the kinematic constraint imposed, then the continuous curve would be comparable to the other two. However, a common input is used to show the impact of the kinematic constraint. We see that the resulting gluon is smaller and less steep. This implies that subleading $\ln(1/x)$ corrections are significant.

4.3 Effect of $\ln(1/x)$ resummation on the structure function F_2

To investigate the various effects of the $\ln(1/x)$ terms we compute $F_2(x, Q^2)$ using four different procedures but with a common input³

$$xg(x, k_0^2) = 1.57(1-x)^{2.5},$$

corresponding to fit 1. The four different determinations are shown in Fig. 6 and correspond to

³In this calculation we have only included the light quarks u, d, s (which we treat as massless), since we want to avoid any dependence on the choice of scale for the heavy quarks. Such a dependence would spoil the clarity of the explanation of some effects which we want to stress. Everywhere else we include also the charm quark.

- (i) The full unified BFKL + GLAP calculation with the kinematic constraint included, eqs.(10) and (45), shown as a continuous curve.
- (ii) Analogous to (i) but without the kinematic constraint (dashed curve).
- (iii) Replace (10) by the pure GLAP equation in the gluon sector, eq. (63), but keep the full k_T factorization for the quarks (dotted curve).
- (iv) Pure GLAP evolution for both the gluons and the quarks (dot-dashed curve). That is instead of (45) we use

$$\begin{aligned} \Sigma(x, k^2) = & S^{(a)}(x) + S^{(b)}(x, k^2) + V(x, k^2) + \\ & \int_x^1 dz P_{qg}(z) \int_{k_0^2}^{k^2} \frac{dk'^2}{k'^2} f\left(\frac{x}{z}, k'^2\right) \xi(k'^2, k^2) \end{aligned} \quad (65)$$

where $\xi(k'^2, k^2)$ is the evolution length and is defined by,

$$\xi(k'^2, k^2) = \int_{k'^2}^{k^2} \frac{dq'^2}{q'^2} \alpha_S(q'^2). \quad (66)$$

One can again see from Fig. 6 that the differences between BFKL (with no kinematical constraint) and GLAP evolution in the gluon sector are not very big. The calculations start to differ only at $x \simeq 10^{-4}$ (dashed and dotted lines). On the other hand when we compare the pure GLAP evolution (with the P_{qg} splitting function) with the equations where the entire phase space has been taken into account then the differences are much bigger. This implies that the leading order terms in $\alpha_S \ln 1/x$ present in the gluon off-shell structure function ($F_2^{\gamma g}$) are much more important than the terms in the gluon anomalous dimension resulting from the BFKL equation. The effect of the kinematic constraint is again evident. It leads to the change from the dashed to the continuous curves. Fig. 6 also enables us to see the x values at which the effect of the $\ln(1/x)$ summation effects become important.

4.4 Predictions for F_2^c and F_L

Once we have determined the parton distributions we can predict the values of other hard scattering observables. At small x we see, via the k_T factorization theorem, that the observables are ‘driven’ by the unintegrated gluon distribution $f(x, k^2)$. Here we calculate F_2^c and F_L .

The charm component F_2^c of F_2 is given by

$$F_2^c(x, Q^2) = e_c^2 S_{q=c}(x, Q^2)$$

where the charm sea $S_{q=c}$ is calculated from (39) in terms of the gluon. It is the second term on the right-hand side of (39) which drives the small x behaviour. The predictions are compared with the H1 measurements [38] of F_2^c in Fig. 7. The percentage of charm in the deep inelastic structure function is shown in Fig. 8. At small x we see that F_2^c is an appreciable fraction of

F_2 . Recall that in the massless charm limit the fraction would be 0.4, provided that we are below the bottom quark threshold.

The predictions of the longitudinal structure function F_L are shown in Fig. 9. For F_L the k_T factorization formula can be written in the form [28, 39]

$$F_L(x, Q^2) = \frac{\alpha_s(Q^2)}{\pi} \left[\frac{4}{3} \int_x^1 \frac{dy}{y} \left(\frac{x}{y} \right)^2 F_2(y, Q^2) + \sum_q e_q^2 \int_x^1 \frac{dy}{y} \left(\frac{x}{y} \right)^2 \left(1 - \frac{x}{y} \right) yg(y, k_0^2) \right] \\ + \sum_q e_q^2 \frac{Q^4}{\pi^2} \int_{k_0^2} \frac{dk^2}{k^4} \int_0^1 d\beta \beta^2 (1 - \beta)^2 \int d^2 \kappa' \alpha_S \left[\frac{1}{D_{1q}} - \frac{1}{D_{2q}} \right]^2 f \left(\frac{x}{z}, k^2 \right), \quad (67)$$

where the quark box variables D_{iq} and κ' are defined in (33). The behaviour of F_L is driven by the gluon through the last term. The argument α_S is taken to be $k^2 + \kappa'^2 + m_q^2$ as before.

5. Conclusions

The natural framework for describing ‘hard’ scattering observables at small x Bjorken x is provided by the gluon distribution $f(x, k_T^2)$ *unintegrated* over its transverse momentum, together with the k_T factorization theorem. At small x it is only to be expected that the k_T dependence should be treated explicitly.

In the leading $\ln(1/x)$ limit, $f(x, k_T^2)$ satisfies the BFKL equation. To make a smooth transition to the larger x domain we have studied a modified equation which treats the leading $\ln(1/x)$ and the leading $\ln(Q^2)$ terms on an equal footing. Moreover, we arrange the equation so that we need only to consider $f(x, k_T^2)$ in the perturbative domain, $k_T^2 > k_0^2$. The integrated gluon distribution $xg(x, k_0^2)$ is the only non-perturbative input that is required. At small x , the singlet quark distribution $\Sigma(x, Q^2)$ is controlled by $f(x, k_T^2)$ through the $g \rightarrow q\bar{q}$ splitting. We therefore extend the formalism to a pair of coupled integral equations for f and Σ which embrace both the BFKL leading $\ln(1/x)$ and GLAP leading $\ln(Q^2)$ contributions in a consistent way. A notable feature of the formalism is that we can retain the full perturbative contribution of the quark box which contributes to the sea distribution for *all* Q^2 . In this way we can isolate the non-perturbative contribution to a (scaling) sea contribution whose general form is known from ‘soft’ physics.

An alternative way to unify the BFKL and GLAP formalisms is based on collinear factorization. It has been shown that we can reduce the (leading twist part of the) BFKL behaviour to collinear form in which the the splitting and coefficient functions contain explicit calculable series of $\alpha_S^m (\alpha_S \ln(1/x))^n$ terms. This approach has attracted much interest. However, in the introduction we stressed the advantage of working with the unintegrated gluon distribution and using the k_T factorization theorem, and we mentioned some of the limitations of the reduction of the BFKL equation to collinear form. Here we simply state some of the points to consider. In the ‘unintegrated’ formalism it is straightforward to identify the perturbative contributions which contribute at *all* Q^2 and so to avoid subsuming them in the input distributions. Second,

there is a natural way to introduce the running of α_S in the BFKL formalism, that has increasing theoretical support, which for sufficiently small x goes beyond the Renormalisation Group behaviour (and so is difficult to implement in the collinear factorization approach). Thirdly, the kinematic constraint along the BFKL ladder is easy to implement in the ‘unintegrated’ formalism. Another point is that the BFKL formalism contains all twists, whereas only the leading twist is retained in the collinear approach. Last, but not least, the k_T factorization approach, which we may symbolically write as $F_2 = F_2^{\gamma g} \otimes f$, is easier to implement. The BFKL kernel and the off-shell gluon structure function $F_2^{\gamma g}$ are calculable perturbatively. We simply use leading order in α_S expressions. The $\ln(1/x)$ summations are implicit in the integration over the *entire* k_T^2 phase space of the gluon ladder and in the k_T factorization integrals.

We solved numerically the coupled integral equations for $f(x, k_T^2)$ and $\Sigma(x, k_T^2)$, and we then used the k_T factorization theorem to calculate F_2 in terms of a two-parameter input form for the gluon, $xg(x, k_0^2) = N(1-x)^\beta$. The parameters N and β are determined by a fit to the available small x data for F_2 . An excellent description is obtained. The data at the smallest values of x give support for the presence of the kinematic constraint, as does the extrapolation of the gluon to describe the WA70 prompt photon data at $x \simeq 0.4$. Notice that the rise of F_2 with decreasing x is purely of perturbative origin in our description, and that we find a significant ‘BFKL’ component.

The fact that we achieve an excellent two-parameter fit of the small x data for F_2 is not, in itself, remarkable. Other equally good phenomenological fits have been obtained. What is encouraging is that we have a theoretically well-grounded and consistent formalism which, with the minimum of non-perturbative input, is able to give a good perturbative description of the observed structure of F_2 . Moreover the BFKL/GLAP components of F_2 are decided by dynamics. In this way we have made a determination of the *universal* gluon distribution, $f(x, k_T^2)$, which can be used, via k_T factorization, to predict the behaviour of other small x observables. We showed the predictions for F_2^c and F_L .⁴

Acknowledgements

We thank R.G. Roberts and R.S. Thorne for valuable discussions.

Two of us (JK and AS) thank the Physics Department and JK thanks also Grey College of the University of Durham for their warm hospitality. This research has been partially supported by the Polish State Committee for Scientific Research (KBN) grant NO 2 P03B 231 08 and the EU under contracts NO CHRX-CT92-0004/CT93-357.

⁴The codes for calculating F_2 are available upon request from a.m.stasto@durham.ac.uk

References

- [1] H1 Collab., S. Aid et al., *Nucl. Phys.* **B420** (1996) 3;
ZEUS Collab., M. Derrick et al., *Z. Phys.* **C69** (1996) 607; *Z. Phys.* **C72** (1996) 399.
- [2] E.A. Kuraev, L.N. Lipatov and V.S. Fadin, *Sh. Eksp. Teor. Fiz.* **72** (1977) 373, (*Sov. Phys. JETP* **45** (1977) 199); Ya. Ya. Balitzkij and L.N. Lipatov, *Yad. Fiz.* **28** (1978) 1597 (*Sov. J. Nucl. Phys.* **28** (1978) 822), J.B. Bronzan and R.L. Sugar, *Phys. Rev.* **D17** (1978) 585; T. Jaroszewicz, *Acta. Phys. Polon.* **B11** (1980) 965.
- [3] L.N. Lipatov, in “Perturbative QCD”, edited by A.H. Mueller (World Scientific, Singapore, 1989), p. 441.
- [4] A.D. Martin, R.G. Roberts and W.J. Stirling, *Phys. Lett.* **B387** (1996) 419.
- [5] CTEQ collaboration: H.L. Lai et al., *Phys. Rev.* **D55** (1997) 1280.
- [6] M. Glück, E. Reya and A. Vogt, *Z. Phys.* **C67** (1995) 433.
- [7] C. Lopez, F. Barreiro, F.J. Yndurain, *Z. Phys.* **C72** (1996) 561.
- [8] S. Catani, M. Ciafaloni and F. Hautmann, *Phys. Lett.* **B242** (1990) 97; *Nucl. Phys.* **366** (1991) 657; J.C. Collins and R.K. Ellis, *Nucl. Phys.* **B360** (1991) 3; S. Catani and F. Hautmann, *Nucl. Phys.* **B427** (1994) 475.
- [9] M. Ciafaloni, *Phys. Lett.* **B356** (1995) 74.
- [10] A.J. Askew, J. Kwiecinski, A.D. Martin and P.J. Sutton, *Phys. Rev.* **D47** (1993) 3775.
- [11] I. Bojak and M. Ernst, Dortmund preprint DO-TH 96/25, hep-ph/9702282.
- [12] A.J. Askew, J. Kwiecinski, A.D. Martin and P.J. Sutton, *Mod. Phys. Lett.* **A8** (1993) 3813; *Phys. Rev.* **D49** (1994) 4402.
- [13] R.S. Thorne, Rutherford preprint, RAL-96-065, January 1997.
- [14] L.N. Gribov, E.M. Levin and M.G. Ryskin, *Phys. Rev.* **100** (1983) 1.
- [15] G. Camici and M. Ciafaloni, hep-ph/9612235.
- [16] G. Camici and M. Ciafaloni, *Phys. Lett.* **B386** (1996) 341; hep-ph/9701303.
- [17] J. Kwiecinski, *Z. Phys.* **C29** (1985) 561; J.C. Collins and J. Kwiecinski, *Nucl. Phys.* **B316** (1985) 307.
- [18] J. Kwiecinski and A.D. Martin, *Phys. Lett.* **B353** (1995) 123.
- [19] E.M. Levin, *Nucl. Phys.* **B483** (1995) 303.

- [20] M. Ciafaloni, *Nucl. Phys.* **B296** (1988) 49; S. Catani, F. Fiorani and G. Marchesini, *Phys. Lett.* **B234** (1990) 18; *Nucl. Phys.* **B336** (1990) 18; G. Marchesini in Proceedings of the Workshop "QCD at 200 TeV", Erice, Italy, (1990) eds. L. Cifarelli and Yu. L. Dokshitzer (Plenum Press, New York, 1992); G. Marchesini, *Nucl. Phys.* **B445** (1995) 49.
- [21] J. Kwiecinski, A.D. Martin and P.J. Sutton, *Phys. Rev.* **D52** (1995) 1445.
- [22] J. Kwiecinski, A.D. Martin and P.J. Sutton, *Z. Phys.* **C71** (1996) 585.
- [23] B. Andersson, G. Gustafson and J. Samuelsson, Lund preprint, LU-TP 95-13; B. Andersson, G. Gustafson, H. Kharraziha and J. Samuelsson, *Z. Phys.* **C71** (1996) 613.
- [24] Yu. L. Dokshitzer et al., *Rev. Mod. Phys.* **60** (1988) 373.
- [25] J. Kwiecinski, A.D. Martin and P.J. Sutton, *Phys. Rev.* **D53** (1996) 6094.
- [26] C. Bottani et al., Milano preprint IFUM 552-FT, hep-ph/9702418.
- [27] A. Donnachie and P.V. Landshoff, *Phys. Lett.* **B296** (1992) 257; *Z. Phys.* **C61** (1994) 161.
- [28] J. Blümlein, *J. Phys.* **G19** (1993) 1623; *Nucl. Phys. B* (Proc. Suppl.) **39B,C** (1995) 22.
- [29] T. Jaroszewicz, *Phys. Lett.* **B116** (1982) 291.
- [30] R.K. Ellis, Z. Kunszt and E.M. Levin, *Nucl. Phys.* **B420** (1994) 517; *erratum* **B433** (1995) 498.
- [31] R.K. Ellis, F. Hautmann and B.R. Webber, *Phys. Lett.* **B348** (1995) 582.
- [32] R.D. Ball and S. Forte, *Phys. Lett.* **B351** (1995) 313.
- [33] J.R. Forshaw, R.G. Roberts and R.S. Thorne, *Phys. Lett.* **B356** (1995) 79.
- [34] J. Blümlein, S. Riemersma and A. Vogt, hep-ph/9607325.
- [35] J. Kwieciński and D. Stozik-Kotlorz, *Z. Phys.* **C48** (1990) 315.
- [36] BCDMS collaboration: A.C. Benvenuti et al., *Phys. Lett.* **B223** (1989) 485; New Muon collaboration (NMC): M. Arneodo et al., *Nucl. Phys.* **B483** (1997) 3; E665 collaboration: M.R. Adams et al., *Phys. Rev.* **D54** (1996) 3006.
- [37] WA70 collaboration: M. Bonesini et al., *Z. Phys.* **C38** (1988) 371.
- [38] H1 collaboration: C. Adloff et al., *Z. Phys.* **C72** (1996) 593.
- [39] B. Badełek, J. Kwieciński and A. Staśto, Durham Preprint, DTP/96/16 (hep-ph/9603230).

Figure captions

- Fig. 1 The diagrammatic representation of the k_T factorization formula $F_i = F_i^{\gamma g} \otimes f$. At lowest order in α_S , the photon-gluon fusion processes (or to be precise the structure functions $F_i^{\gamma g}$ of the virtual gluon) are given by the quark box shown (together with the crossed box).
- Fig. 2 The two-parameter fit to the F_2 data at small x using eq. (10) for $f(x, k^2)$ with (continuous curves) and without (dashed curves) the kinematic constraint. The optimum values of the parameters N and β , which describe the input form of the gluon, are given in Table 1. The figure shows the H1 data [1] together with the E665 and NMC measurements [36] which occur at the same values of Q^2 .
- Fig. 3 As for Fig. 1, but for the ZEUS measurements [1] of F_2 , together with the E665, NMC and BCDMS data [36] which occur at the same values of Q^2 .
- Fig. 4 The continuous curves show the behaviour of the conventional gluon distribution $xg(x, Q^2)$ corresponding to fit 1, and calculated using eq. (1). For comparison we also show the gluon distributions of the MRS (R2) [4] (dashed curve) and GRV [6] (dotted curve) sets of partons.
- Fig. 5 The unintegrated gluon distribution $f(x, k^2)$ as a function of k^2 for $x = 10^{-4}$ and 10^{-3} obtained by solving the simultaneous equations for $f(x, k^2)$ and $\Sigma(x, k^2)$. The continuous and dashed curves are obtained by using the unified BFKL/GLAP equation (10) for $f(x, k^2)$ with and without the kinematic constraint respectively. The dotted curve corresponds to using GLAP evolution for f , eq. (63). In each case the input $xg(x, k_0^2) = 1.57(1-x)^{2.5}$ is used, where $k_0^2 = 1\text{GeV}^2$.
- Fig. 6 The light quark contribution to $F_2(x, Q^2)$ for various Q^2 values obtained from solving different sets of coupled equations for the gluon f and the quark singlet Σ with, in each case, the input $xg(x, k_0^2) = 1.57(1-x)^{2.5}$ where $k_0^2 = 1\text{GeV}^2$. The continuous and dashed curves come from solving (10, 45) with and without the kinematic constraint. The dotted curve is obtained using GLAP in the gluon sector, that is (63,45), whereas the dot-dashed curve corresponds to pure GLAP evolution, (63,65).
- Fig. 7 The predictions for F_2^c , compared with H1 charm data, obtained from the optimum fit (fit 1).
- Fig. 8 Ratio F_2^c/F_2 for different values of Q^2 obtained from fit 1.
- Fig. 9 The prediction for the structure function F_L as a function of x for different values of Q^2 using the parameters of fit 1.

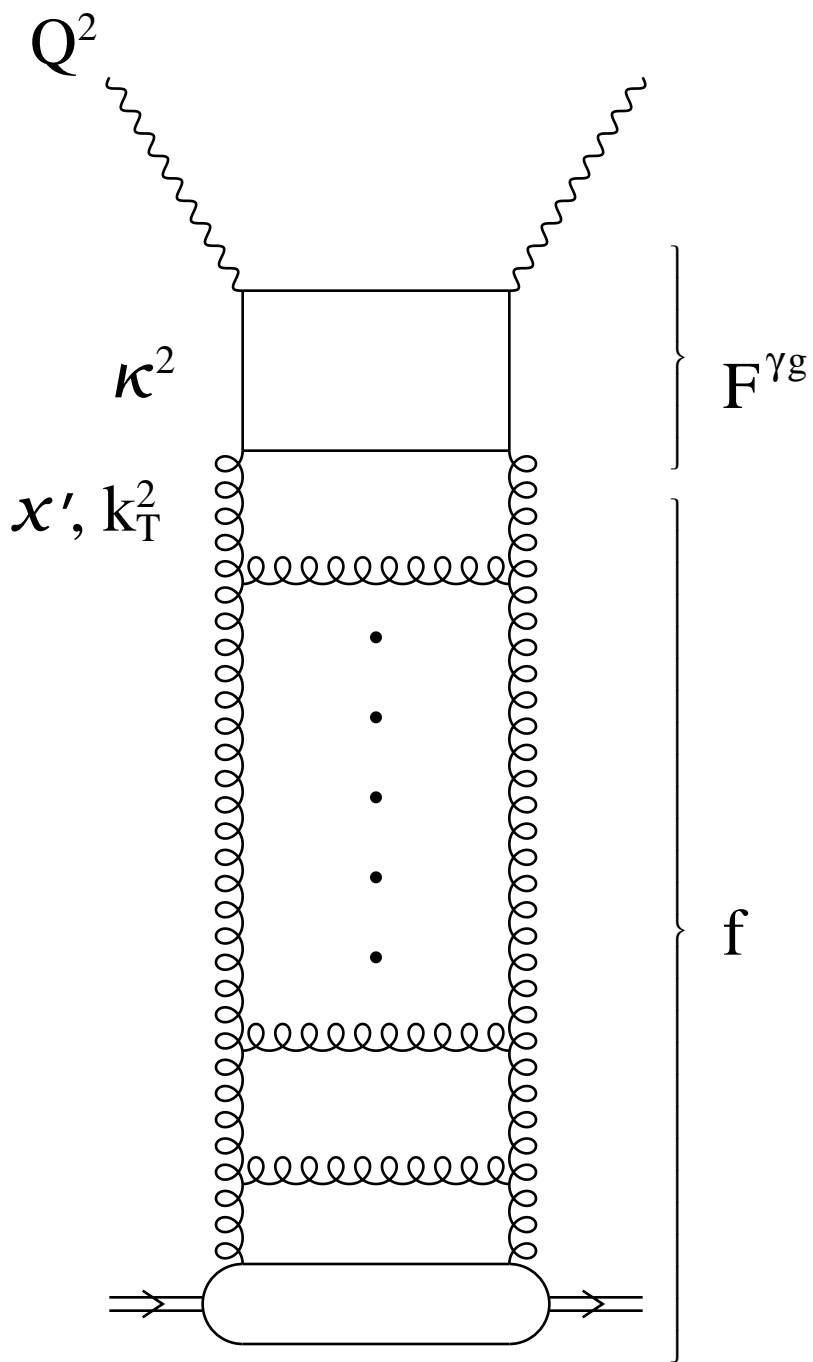


Fig.1

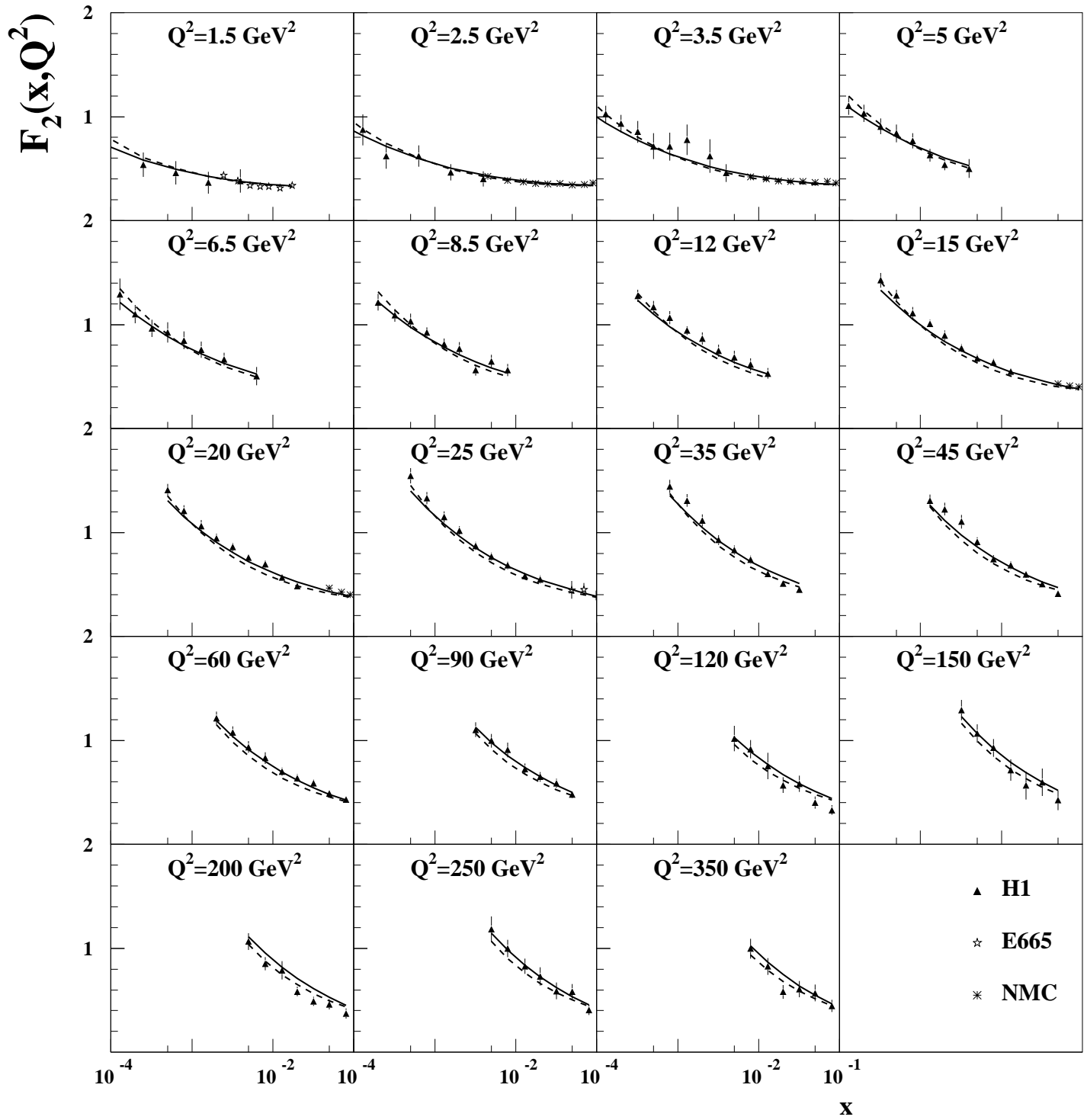


Fig.2

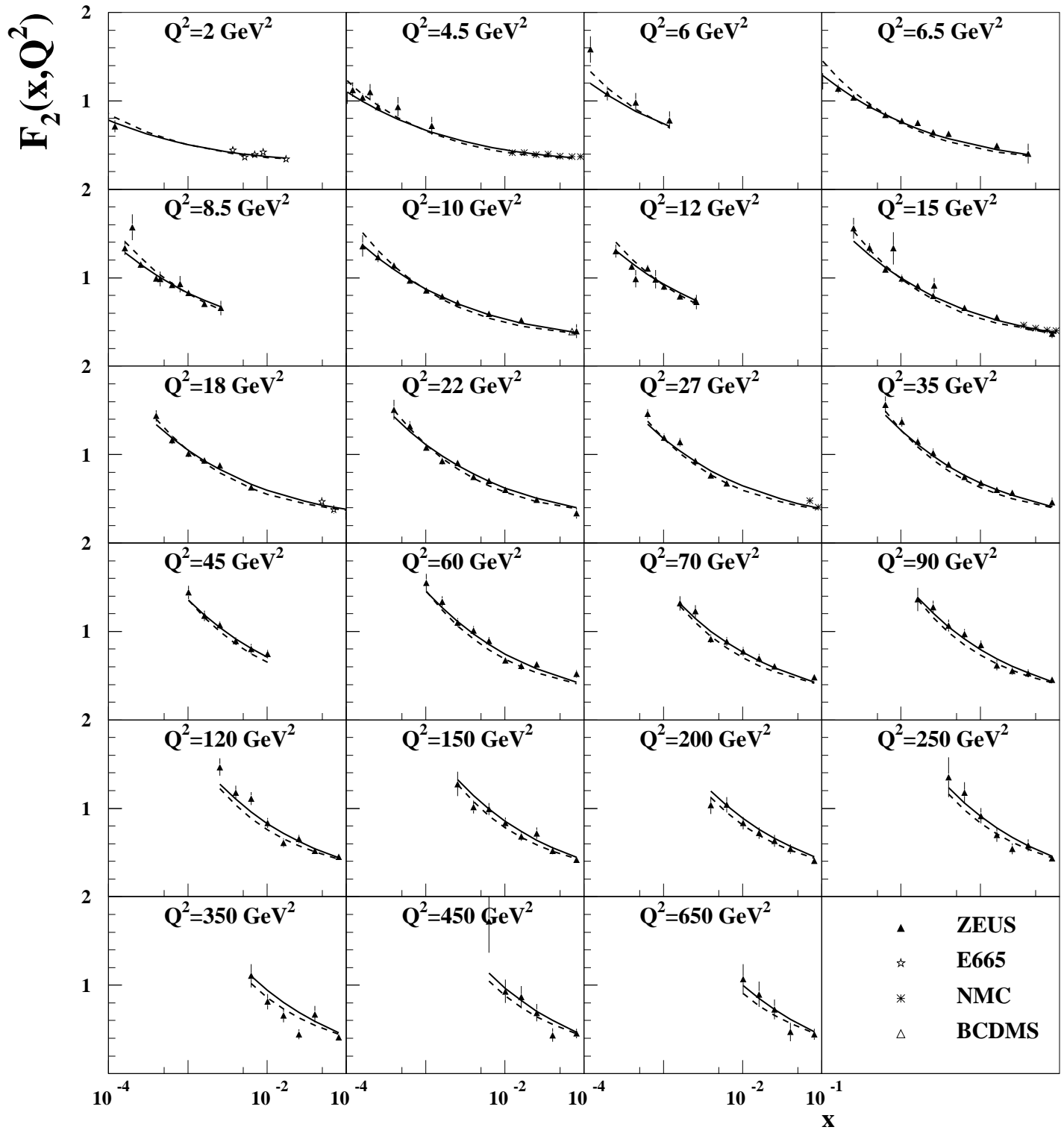


Fig.3

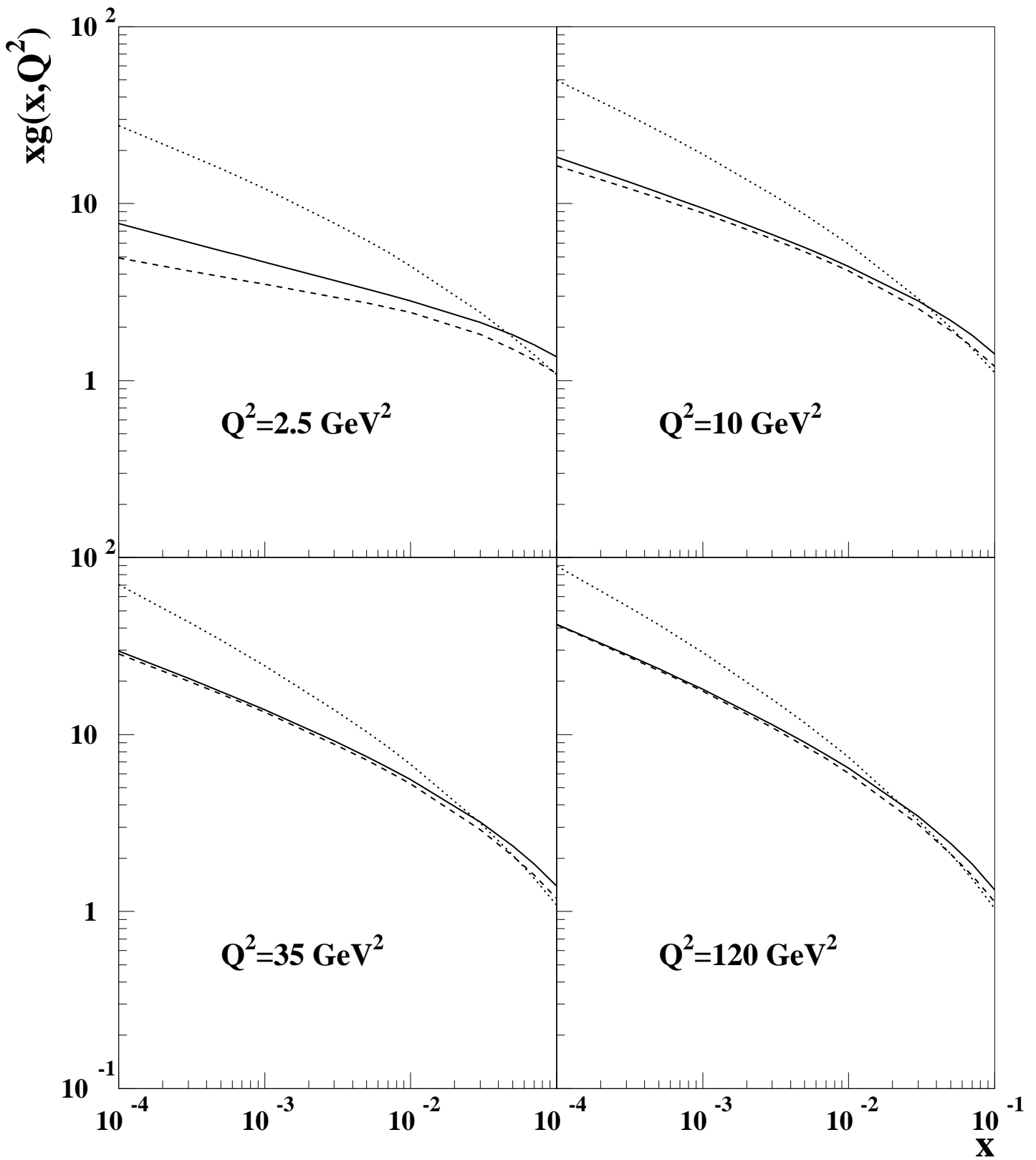


Fig.4

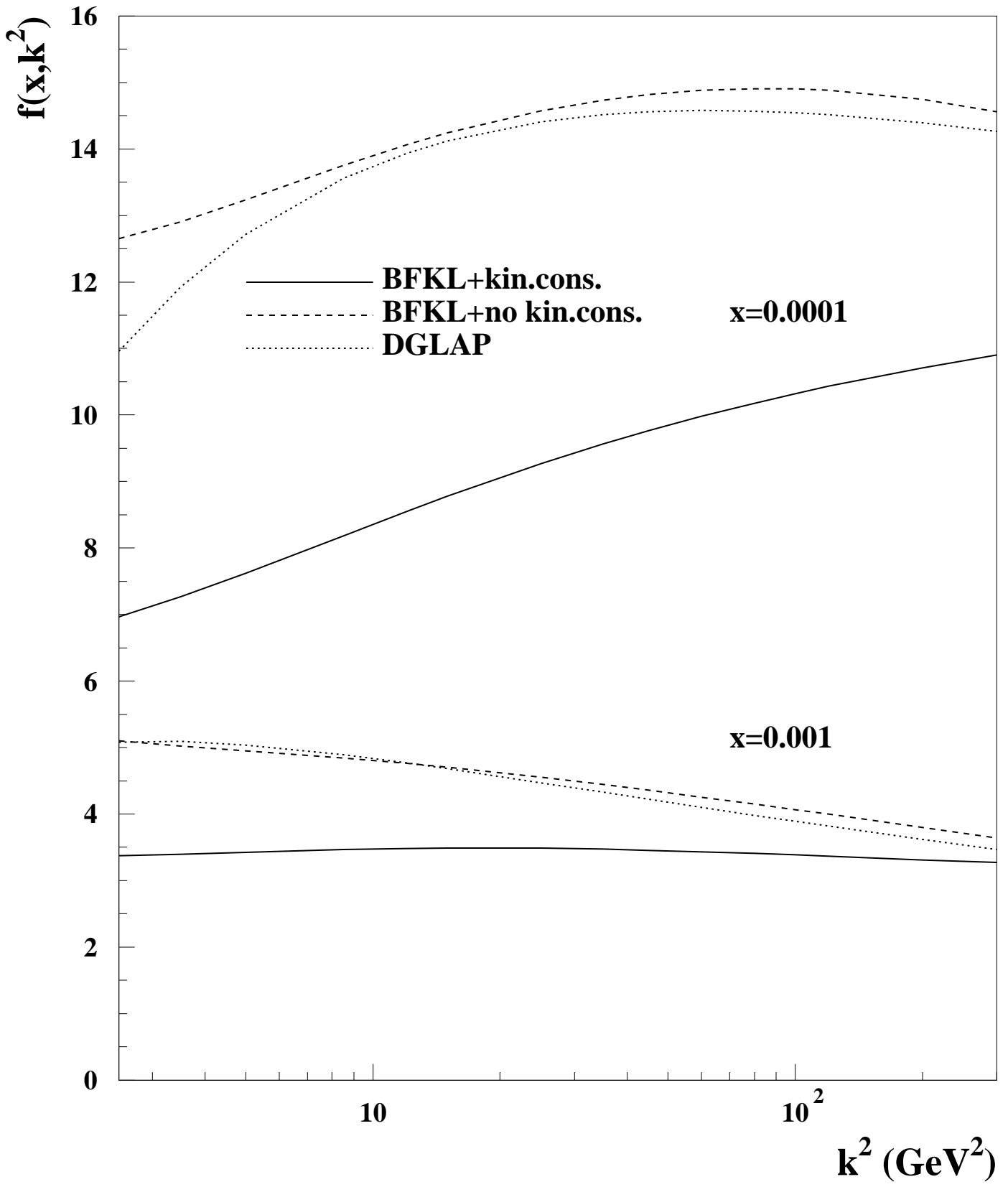


Fig.5

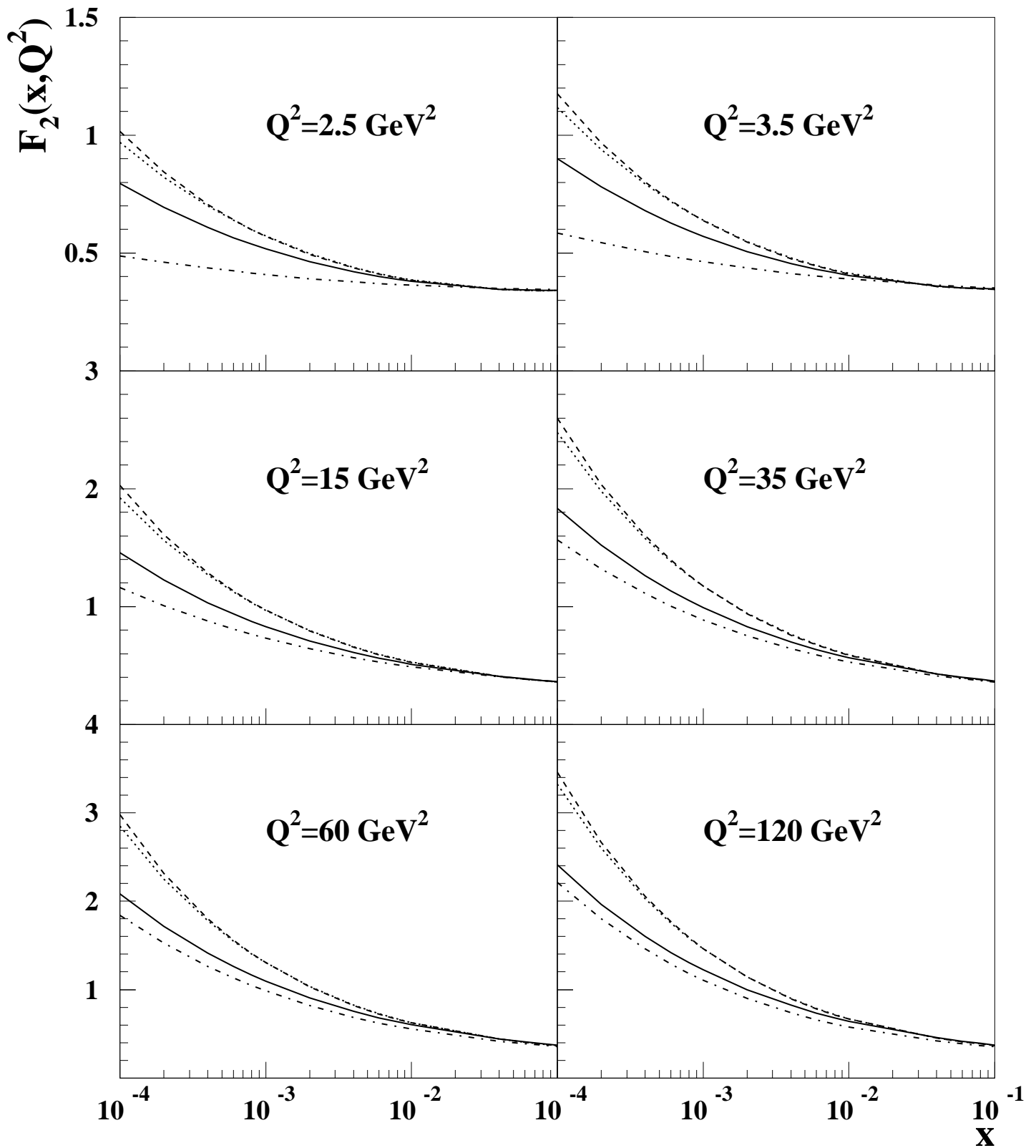


Fig.6

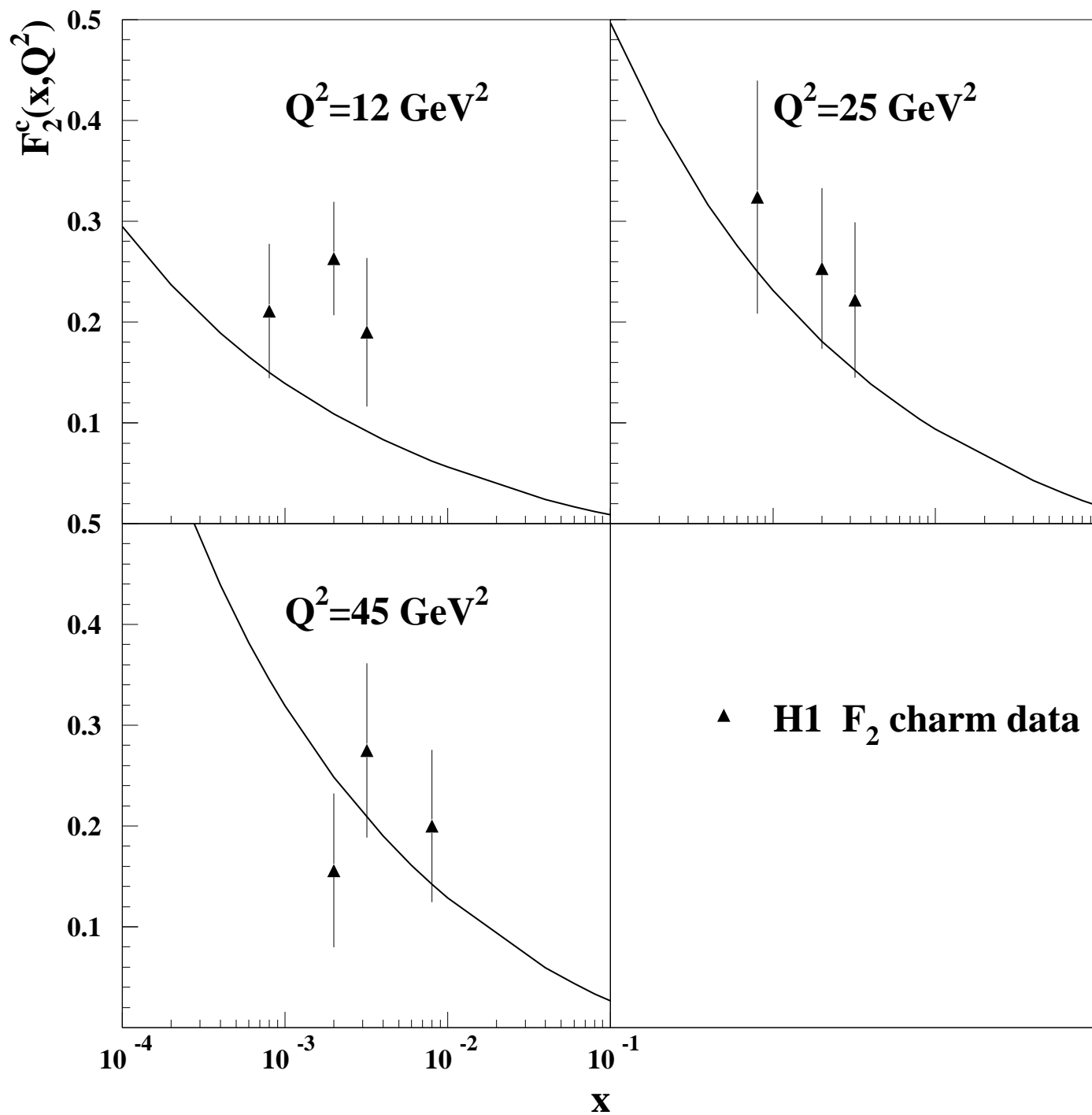


Fig.7

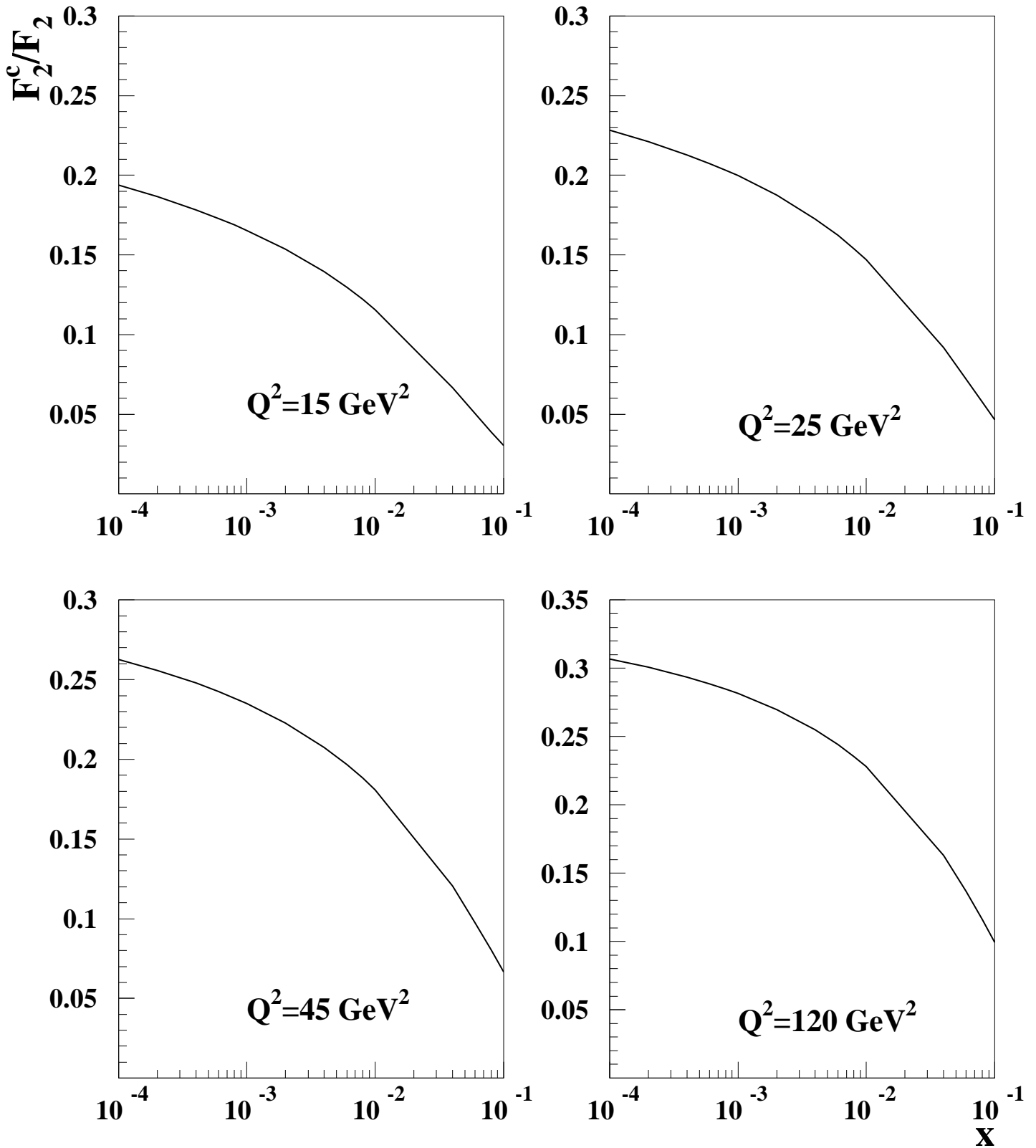


Fig.8

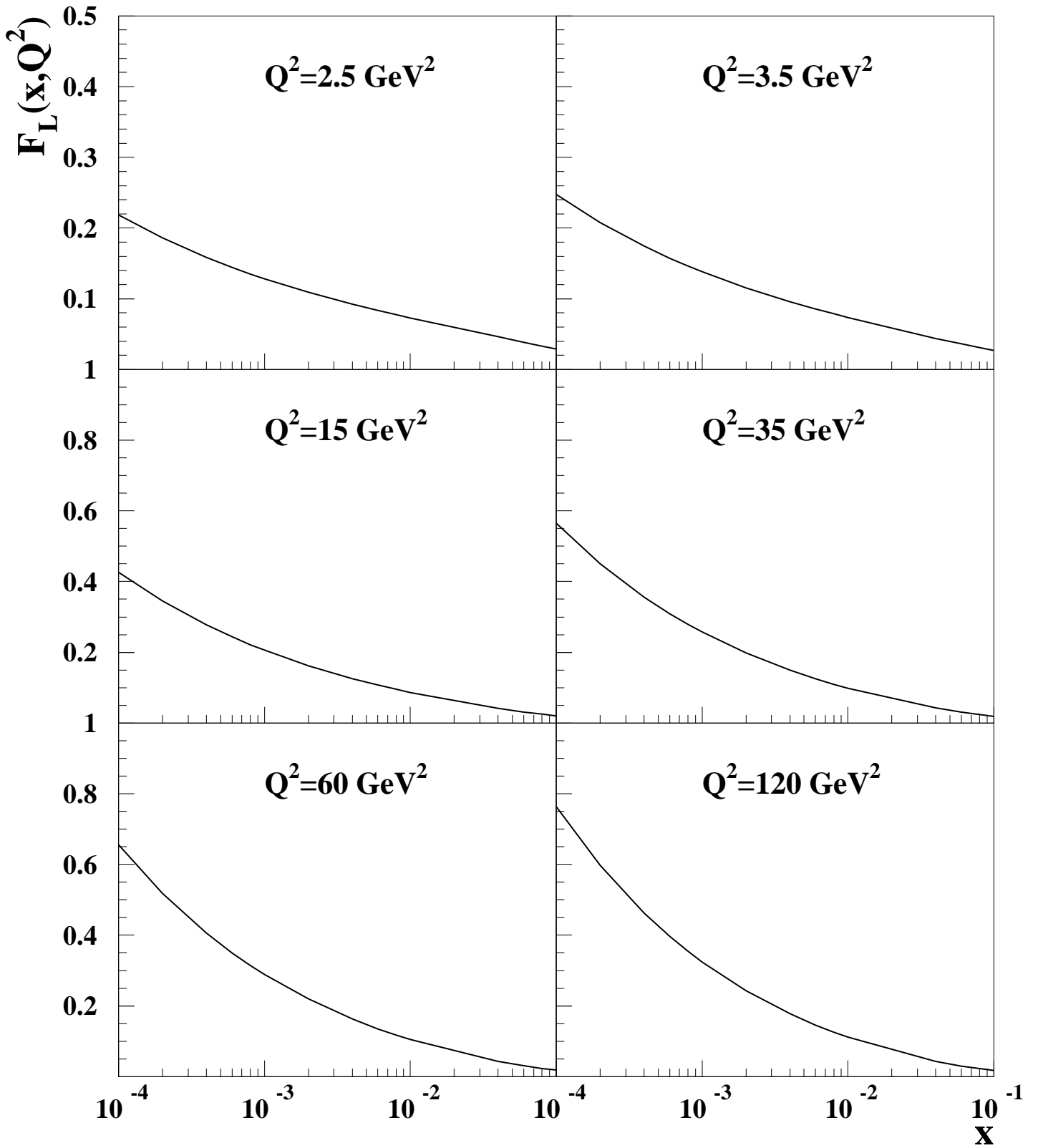


Fig.9